Measurement of Differential Drell–Yan Cross Sections with 190-GeV Pion Beams in COMPASS Experiment at CERN

Speaker : Chia-Yu Hsieh

Department of Physics, Academia Sinica

Outline

- **Introduction**
- Pion-induced Drell-Yan Process
- Pion PDFs

- **Drell-Yan Cross Section Analysis**
- COMPASS Setup
- Drell-Yan Cross Section for NH3, W, and Al targets
- Nuclear Effect (A dependence)

- **Summary and Outlook**

Pion-Induced Drell-Yan Process

Pion-Induced Drell-Yan Process

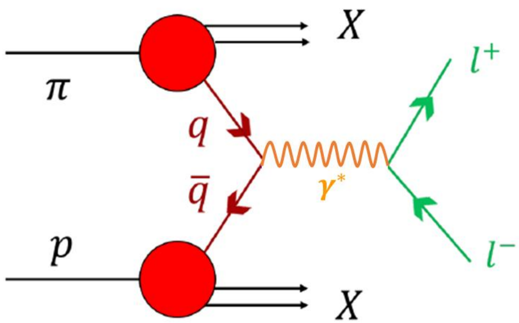

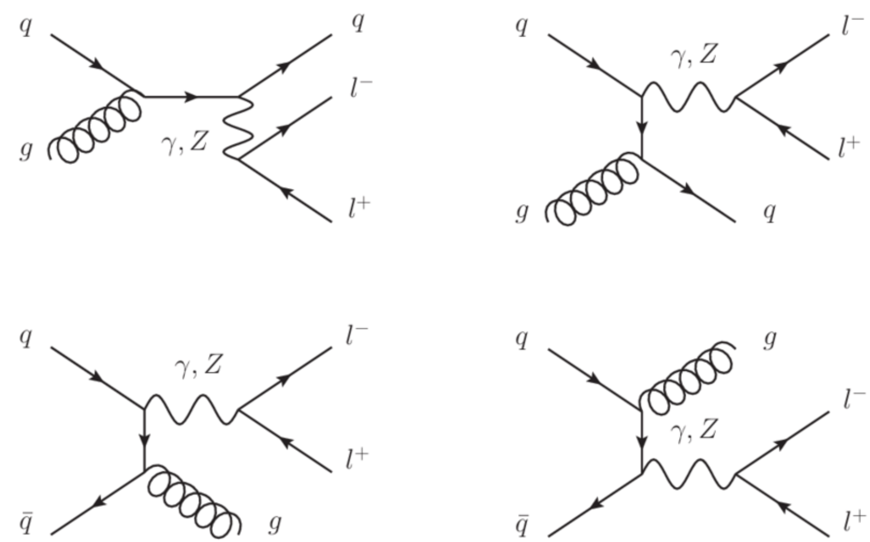

$\boldsymbol{LO \quad : \; q\bar{q} \rightarrow \gamma^{*} \rightarrow l^{+}l^{-}}$

$\boldsymbol{NLO : \; q\bar{q}g \rightarrow \gamma^{*} \rightarrow l^{+}l^{-}g, \qquad qg \rightarrow \gamma^{*} \rightarrow l^{+}l^{-}q}$

S.D. Drell and T.M. Yan
PRL 25 (1970) 316

$$\frac{d^2\sigma}{dM_{ll'}dx_F} = \frac{2\pi\alpha^2}{9M_{ll'}^3}\left(\frac{x_\pi x_p}{x_\pi + x_p}\right)\sum Q_q^2\left[q(x_\pi)\bar{q}(x_p) + \bar{q}(x_\pi)q(x_p)\right]$$

PDF

Journal of High Energy Physics
Article number: 90 (2019)

$$\frac{d^3\sigma}{dM_{ll}dx_F\,\boldsymbol{dp_T}} = \sigma_0 \sum_{f_\pi, f_p} H_{f\pi fp}(M_{ll}, \mu) \int \frac{d^2\boldsymbol{b}}{4\pi} e^{i(\boldsymbol{b}.\boldsymbol{p_T})} F_{h\pi \to f\pi}(x_\pi, \boldsymbol{b}; \mu, \zeta_1) F_{hp \to fp}(x_p, \boldsymbol{b}; \mu, \zeta_1)$$

TMD

$*\ \boldsymbol{transverse\ momentum\ k_T, q_T, p_T}$

Drell-Yan process is an power tool to probe PDF and TMD of pion.

Pion PDF Sets

PDF	Year	pQCD Cal.	Q-evl.	Ref.
OW	1984	LO	Yes	[11]
ABFKW	1989	NLO	Yes	[12]
SMRS	1992	NLO	Yes	[15]
GRV/GRS	1992/1999	NLO	Yes	[13]/ [14]
JAM	2018	NLO	Yes	[16]
xFitter	2020	NLO	Yes	[18]

PDF	Data Used			
	Pion-induced Drell-Yan	Pion-induced J/ψ	Pion-induced prompt-γ	LN-DIS
OW	NA3, WA39	NA3, E537	-	-
ABFKW	NA3, NA10, E537, E615	NA3, E537	WA70, NA24	-
SMRS	NA10, E615	-	WA70	-
GRV/GRS	NA10, E615	-	WA70	-
JAM	NA10, E615	-	-	HERA
xFitter	NA10, E615	-	WA70	-

The pion PDF is mainly extracted from πN scattering which has limited statistics. At 2018, leading-neutron DIS data recently joins the global fit of pion PDF.

Drell – Yan

$\pi^{\pm}p \rightarrow \mu^{+}\mu^{-}X$

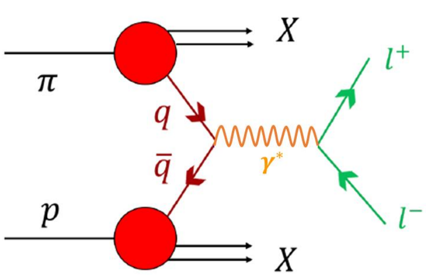

sensitive to valance

J/ψ

$\pi^{\pm}p \rightarrow J/\psi\, X$

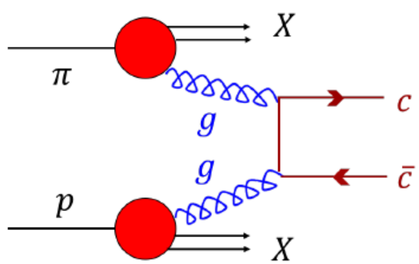

sensitive to gluon

prompt – gamma

$\pi^{\pm}p \rightarrow J/\psi\, X$

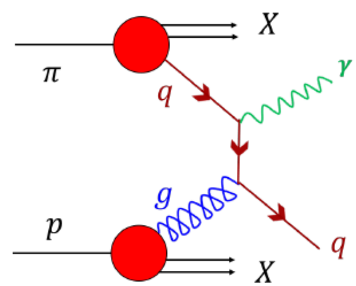

sensitive to gluon

Leanding – neutron DIS

$ep \rightarrow nX$

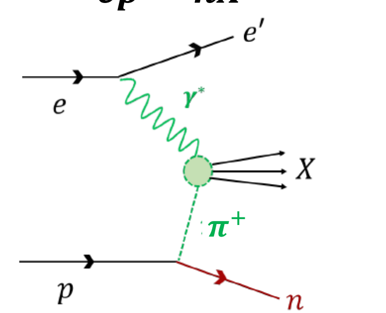

sensitive to quark and gluon

Pion PDF Sets

$Q^2 = 9.6GeV$

Valence | **Sea** | **Gluon**

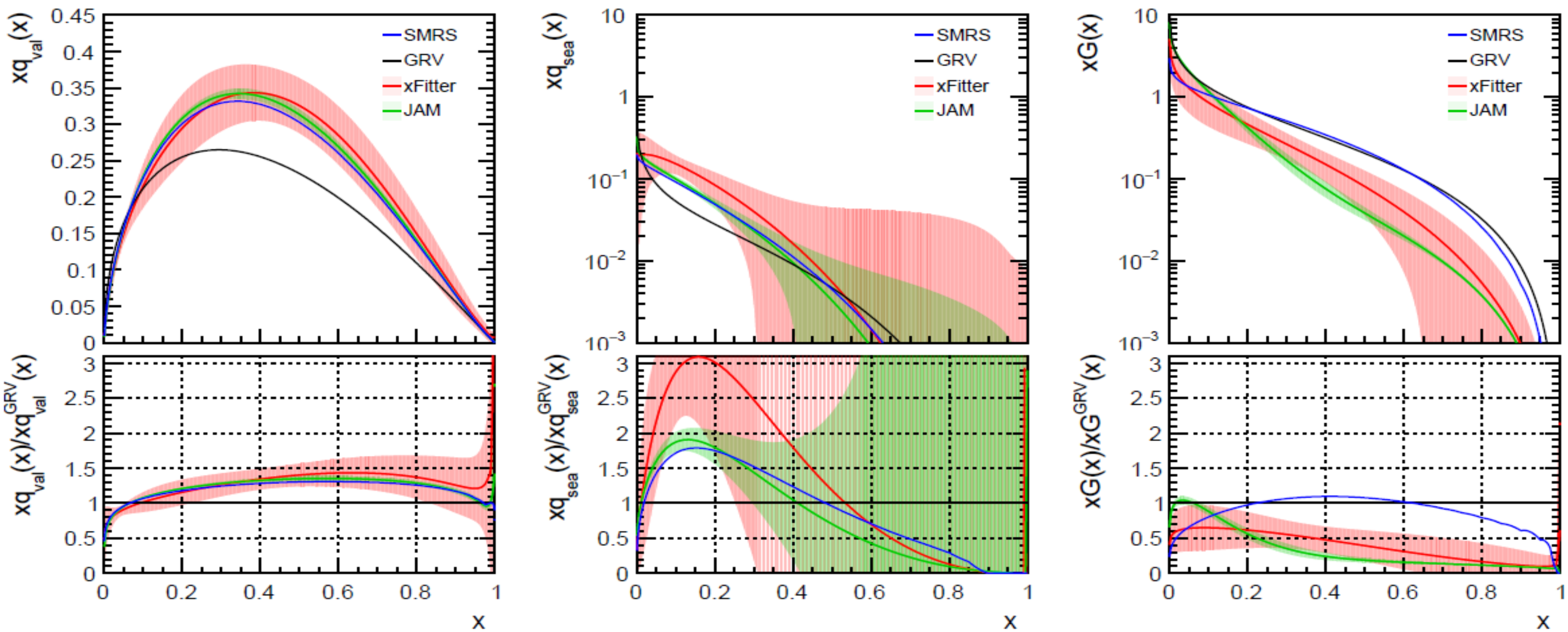

GRV is lower than the others by 30%-50% for valence PDF

Poorly constrained for sea PDF.

GRV and SMRS has larger gluon contamination than JAM and xFitter at $x_\pi > 0.1$

Phys. Rev. D 102, 054024 (2020)

Pion PDF is not as well defined as proton PDF. There are still many puzzles.

COMPASS Experiment

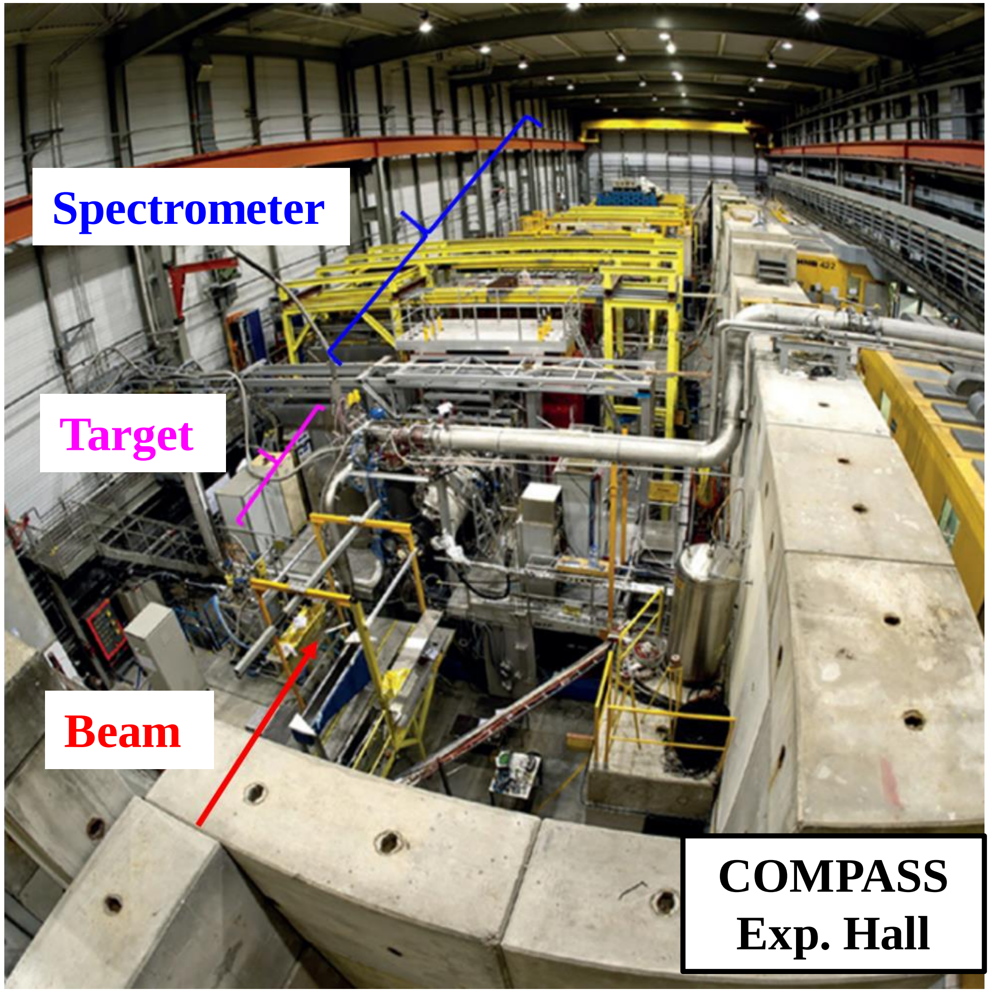

- **A fixed target experiment** at CERN on Prévessin site.

- **COMPASS**
- **A 60m-long spectrometer**
- **Multiple beam choice**

① 160GeV and 200GeV muon
② 190 GeV positive hadron
③ 190 GeV negative hadron

- **Multiple target choice**

① Unpolarized nuclear targets
② Longitudinal and transverse polarized ammonia target.
③ Longitudinal polarized liquid hydrogen target.

- COMPASS is a high flexibility facility to study multiple physics programs
- Pion induced DY : PDF, TMD, nucleon spin.
- DVCS : GPD
- Hadron spectroscopy.

The high flexibility of COMPASS in terms of target and beam allows it to study various physics program.

2015 and 2018 Drell-Yan Data Taking COMPASS

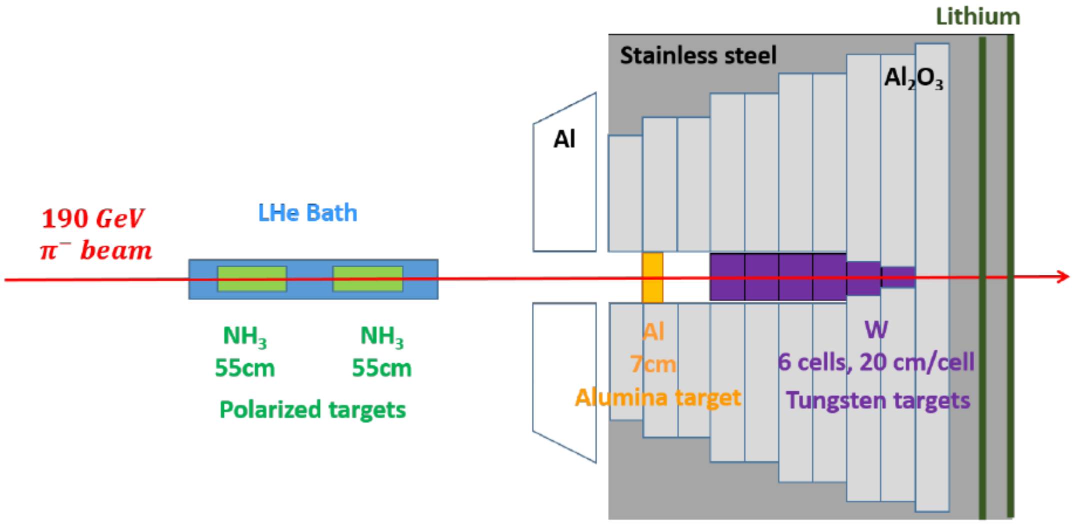

$\pi^- + p \rightarrow \mu + \mu^- + X$

π^- beam | NH_3, Al, W targets | Dimuon events | Hadron absorber

- **Beam** : 190 GeV π^-
- **Target :**

Polarized ammonia targets(PT), Al, W

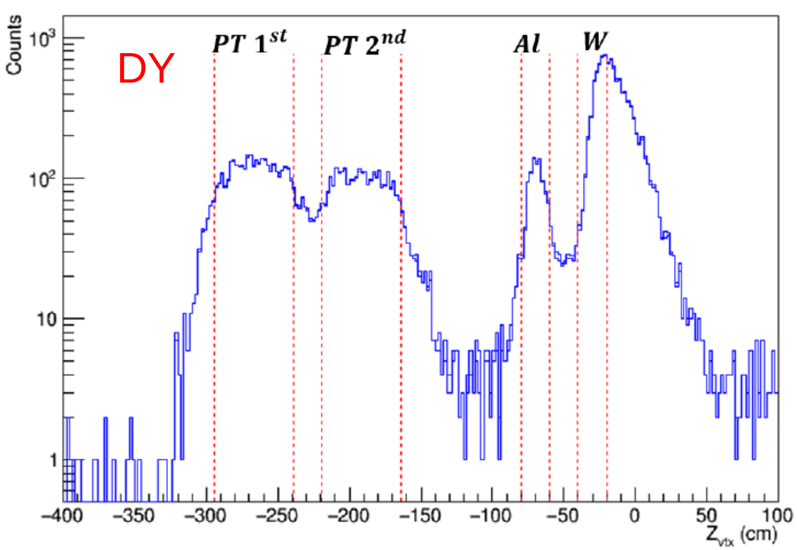

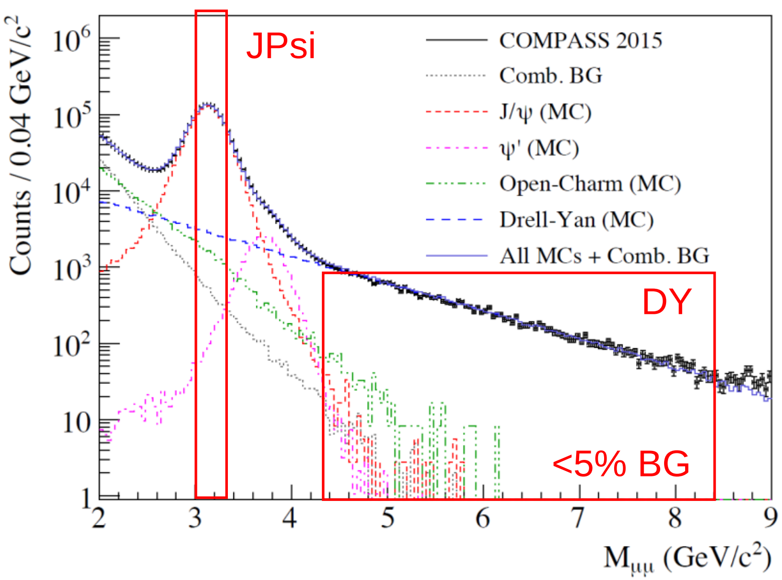

DY Cross-Section Measurement in COMPASS

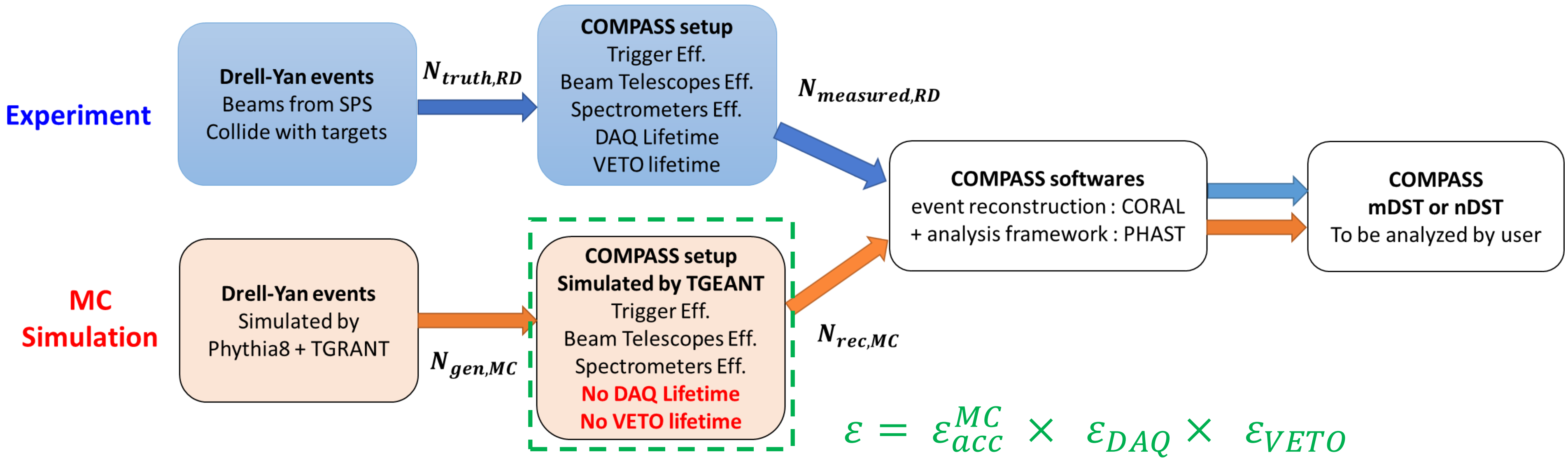

$$\varepsilon = \varepsilon_{acc}^{MC} \times \varepsilon_{DAQ} \times \varepsilon_{VETO}$$

Dimuon Events, N_i

Kinematics, x

$$[\sqrt{\tau}, x_F, p_T], \sqrt{\tau} = M_{\mu\mu}/\sqrt{s}$$

$$\frac{d^2\sigma}{dx_F d\sqrt{\tau}}, \frac{d^2\sigma}{dp_T d\sqrt{\tau}}, \frac{d^2\sigma}{dx_F dp_T}$$

$$\frac{d^n\sigma}{dx_n} = \frac{1}{\mathcal{L}} \times \frac{d(N_i/\varepsilon_i)}{dx_n}$$

Efficiencies, ε

① $\varepsilon_{acc,i}^{MC}$ $[trigger, target, period]$

② $\varepsilon_{VETO,i}[trigger, spill]$

③ $\varepsilon_{DAQ,i}$ $[spill]$

Luminosity, $\mathcal{L}$

① *flux estimation*

② *target density*

COMPASS Dimuon Triggers

Formation of single muon trigger : LAS

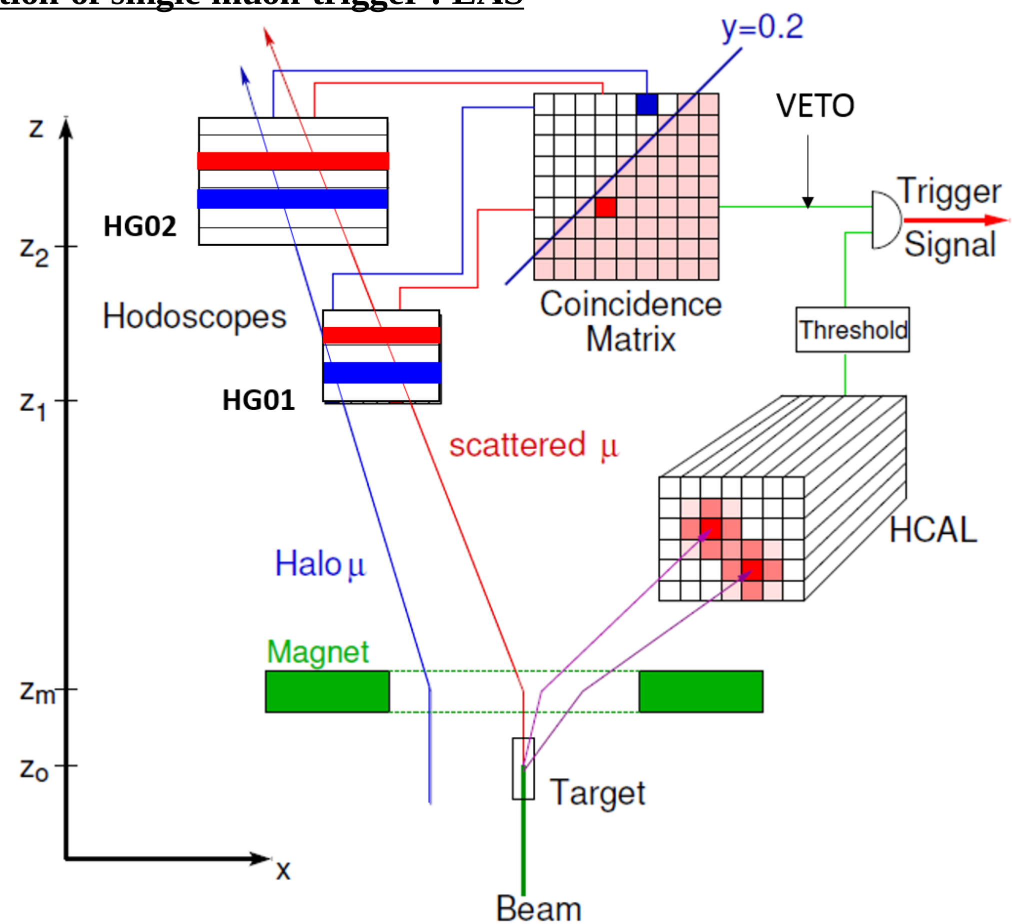

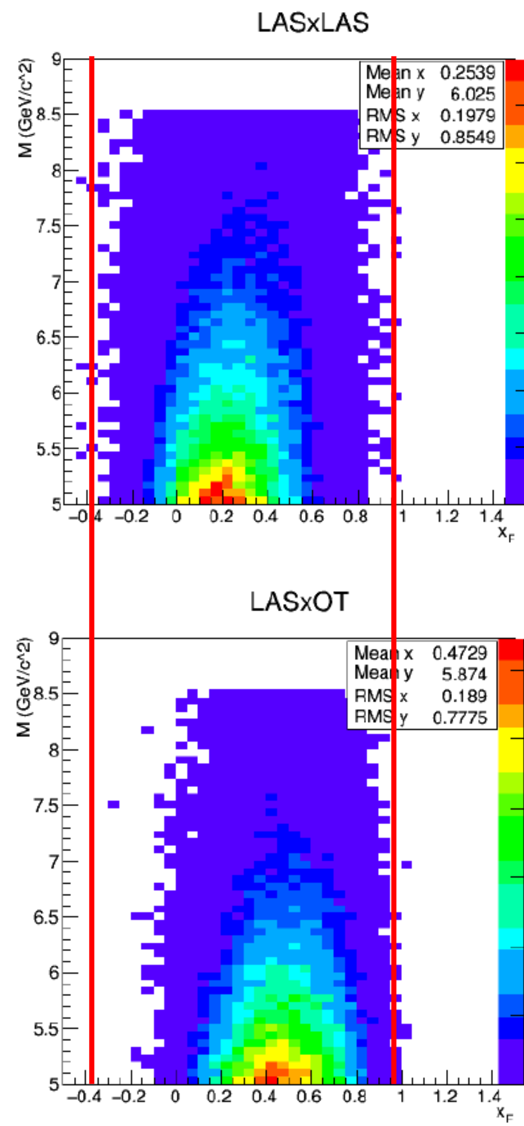

- **Beam VETO**

inhibits muon tracks not interacting with targets.

- **Single muon triggers**

① LAS = HGO1 x HG02

② OT = HO03 x HO04

- **Dimuon triggers**

① LASxLAS (low x_F)

② LASxOT (large x_F)

Luminosity $\mathcal{L}$

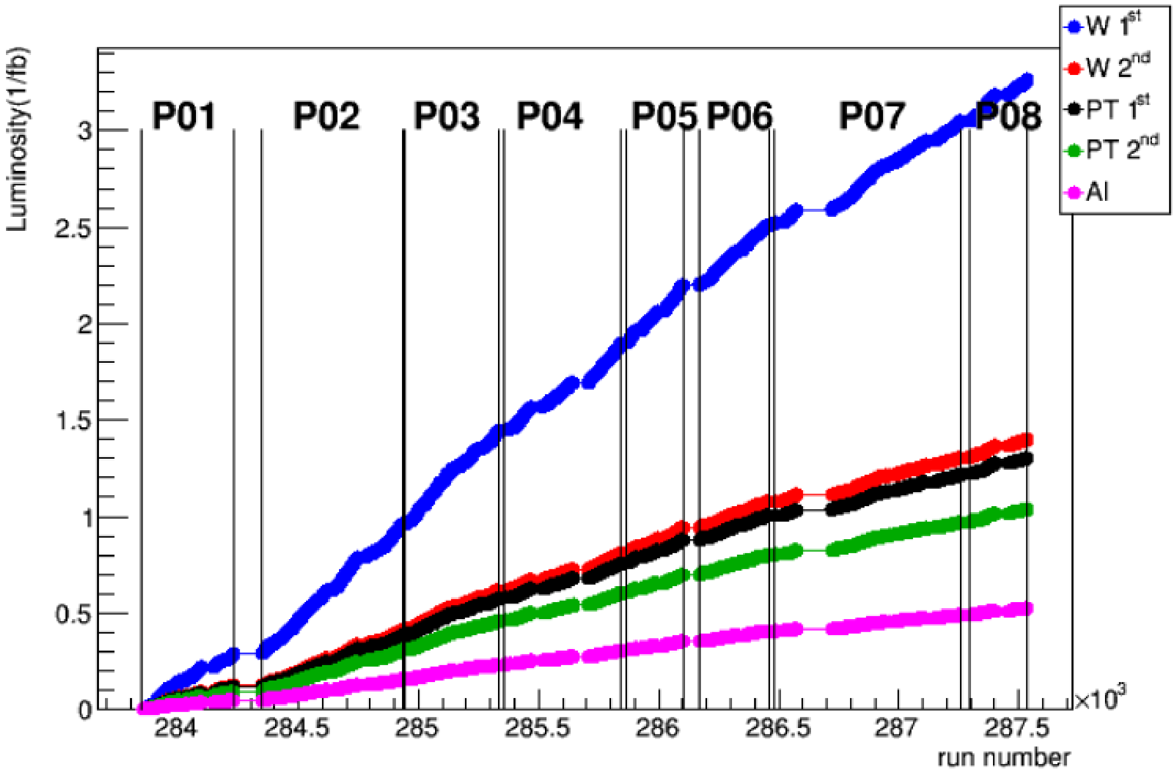

Luminosity in 2018 DY data-taking

① W cells ~ 4.0(1/fb)

② PT cells ~ 1.5 (1/fb)

③ Al cell ~ 0.5 (1/fb)

Comparison between Real Data and MC

W cells

LASxLAS

LASxOT

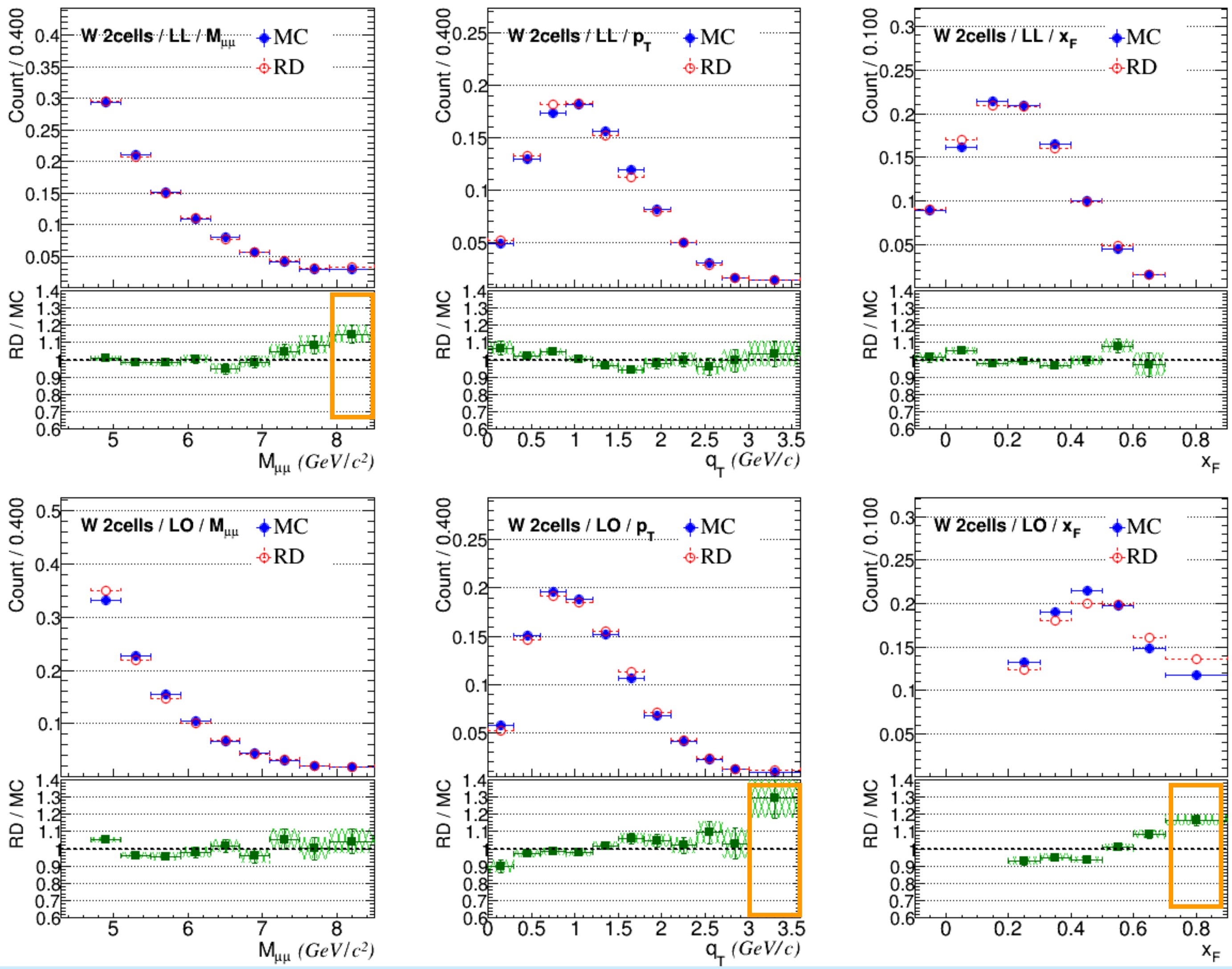

A nice MC and RD consistency is achieved except for some regions with small statistics.

Drell-Yan Cross-Section in $d^2\sigma/dx_\mathrm{F}\, d\sqrt{\tau}$

Pion-Induced Drell-Yan Process

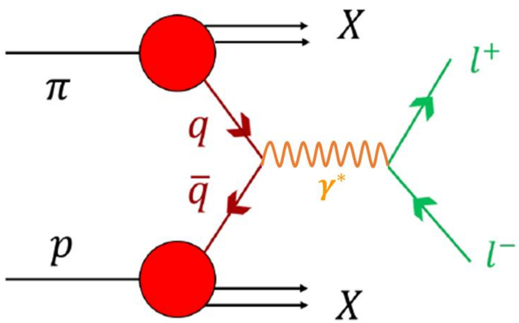

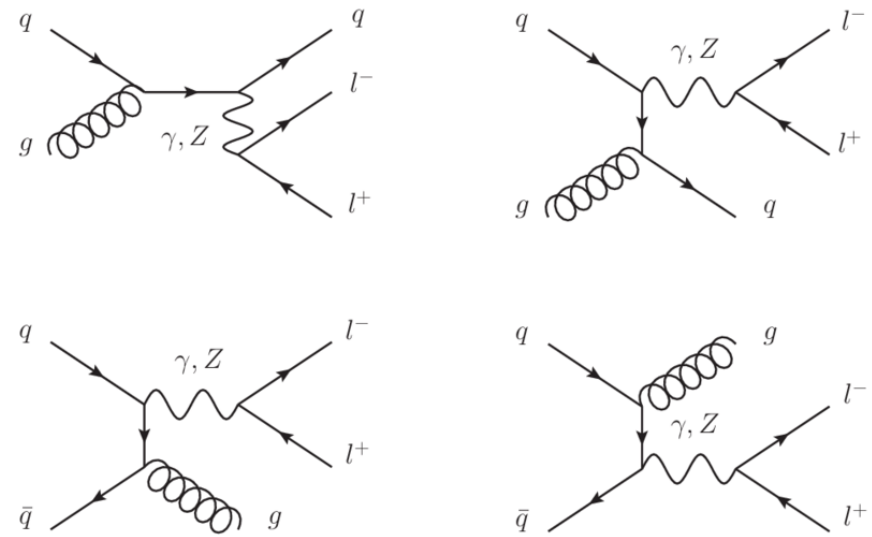

$\boldsymbol{LO} \quad : \boldsymbol{q\bar{q} \rightarrow \gamma^* \rightarrow l^+ l^-}$

$\boldsymbol{NLO} : \boldsymbol{q\bar{q}g \rightarrow \gamma^* \rightarrow l^+ l^- g}, \quad \boldsymbol{qg \rightarrow \gamma^* \rightarrow l^+ l^- q}$

S.D. Drell and T.M. Yan
PRL 25 (1970) 316

$$\frac{d^2\sigma}{dM_{ll'} dx_F} = \frac{2\pi\alpha^2}{9M_{ll'}^3}\left(\frac{x_\pi x_p}{x_\pi + x_p}\right)\sum Q_q^2\,[q(x_\pi)\bar{q}(x_p) + \bar{q}(x_\pi)q(x_p)]$$

PDF

- Drell-Yan Cross-Section in $d^2\sigma/dx_\mathrm{F}\, d\sqrt{\tau}$ is the main input of the global fit of pion PDF.
- Energy scaling : $M_{ll}^3 \frac{d^2\sigma}{dM_{ll'} dx_F} = \frac{M_{ll'}^3}{\sqrt{s}} \frac{d^2\sigma}{d\sqrt{\tau} dx_F}$ is independent of the CM energy of the experiment.

Past Pion-induced Data in $d^2\sigma/dx_F\, d\sqrt{\tau}$

J. Phys. G: Nucl. Part. Phys. 19 D1 (1993)

The **pQCD calculation in NLO** is performed with nucleon PDF of MRS and pion PDF of SMRS in this paper.

E615 @$0.185 < \sqrt{\tau} < 0.208$

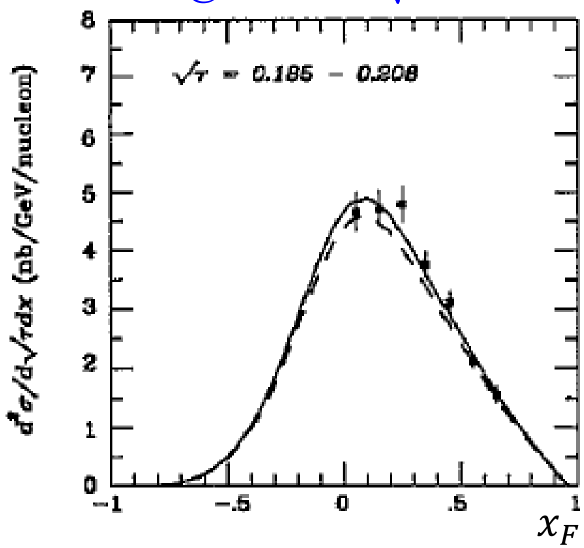

E615 252 GeV pion + W

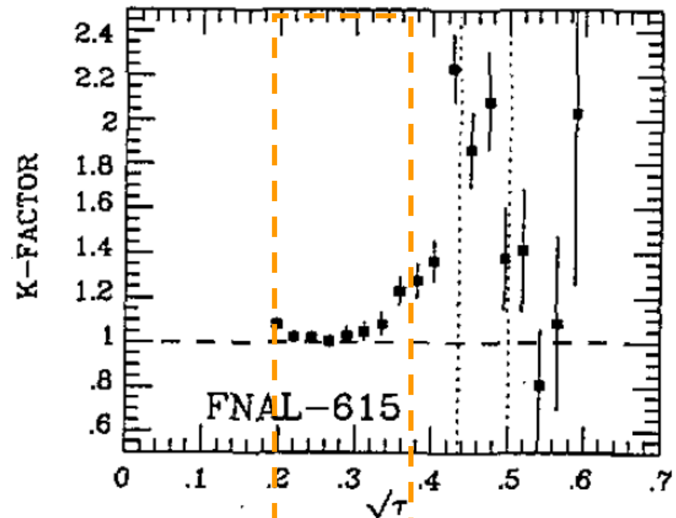

NA10 194 GeV pion + W

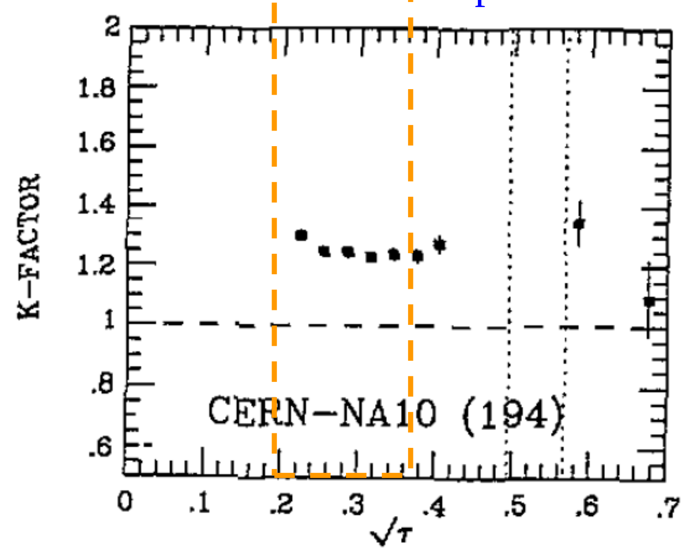

A nice agreement achieved between data and calculation with a small deviation defined as K-factor equal to the ratio between data and calculation :

$$K\ factor = Data/pQCD_{NLO}$$

There is a obvious **normalization issue around 20% between the results given by E615 and NA10** which are the ones used the most in pion PDF global analysis.

Comparison between COMPSS and NA10

W cells

COMASS 190GeV $\pi^- + W$
NA10 194GeV $\pi^- + W$

NA10 data :
Z. Phys. C - Particles and Fields 28 (1985)
J. Phys. G - Nucl. Part. Phys. 19 D1(1993)

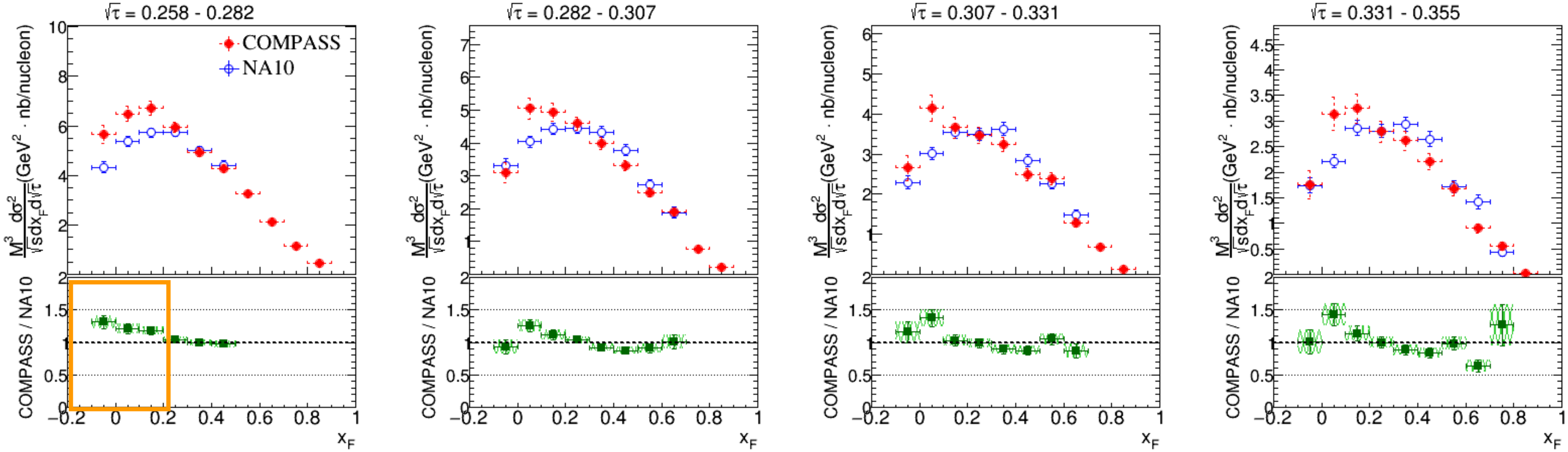

* $\sqrt{\tau} = M_{\mu\mu}/\sqrt{s}$ is the energy fraction of dimuon respect to the energy of πN system.

* Energy scaling of DY cross section : $M_{ll}^3 \frac{d^2\sigma}{dM_{ll'}dx_F} = \frac{M_{ll'}^3}{\sqrt{s}} \frac{d^2\sigma}{d\sqrt{\tau}dx_F}$

- COMPASS data and NA10 data are in nice consistency except for the low x_F region.
- The inconsistency in low x_F region could be caused by the unrealistic MC, multidimensional comparison between RD and MC will be investigated.
- COMPASS data has wider kinematic coverage but less statistics compare to NA10.

Comparison between COMPSS and E615

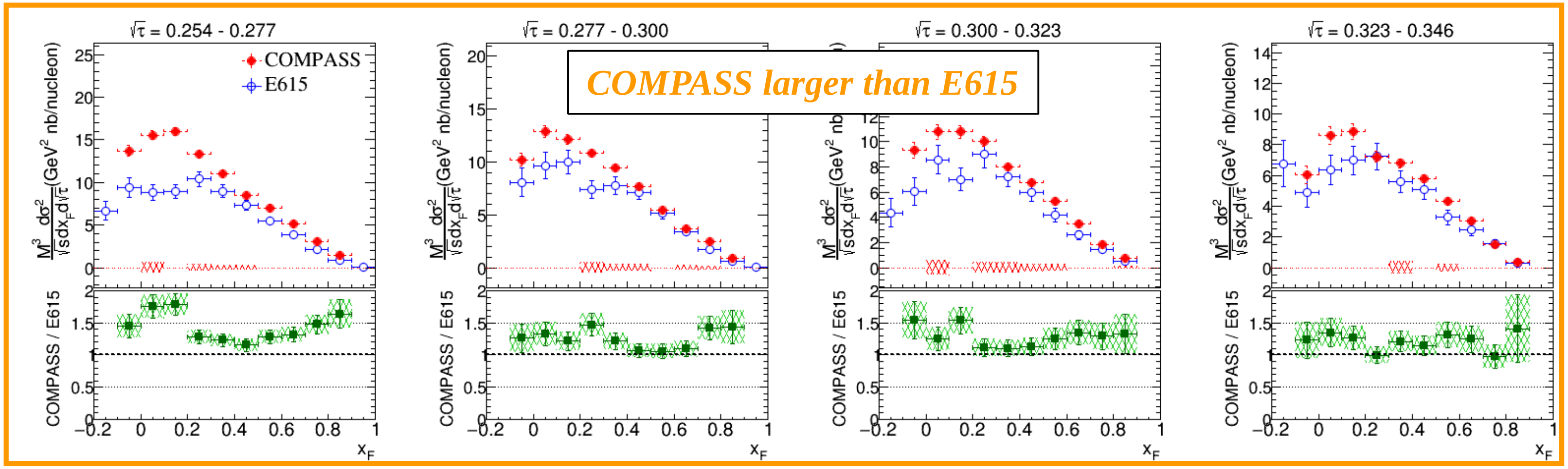

W cells

Kinematics overlapped region between COMPASS, NA10, and E615.

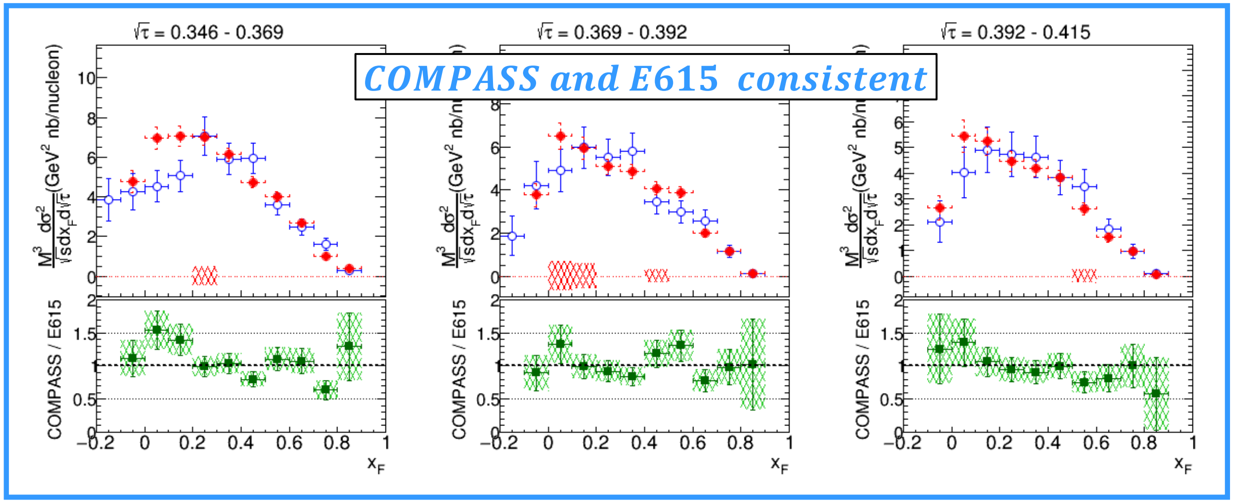

COMASS
190GeV π^- + W
E615
252GeV π^- + W

E615 data : Phys. Rev. D 39 (1989) 92

COMPASS data is larger than E615 data around 10%-50% in the low mass region but consistent with E615 in the higher mass region. COMPASS data have similar kinematic coverage as E615 but better statistics uncertainty.

Comparison with pQCD NLO Calculations

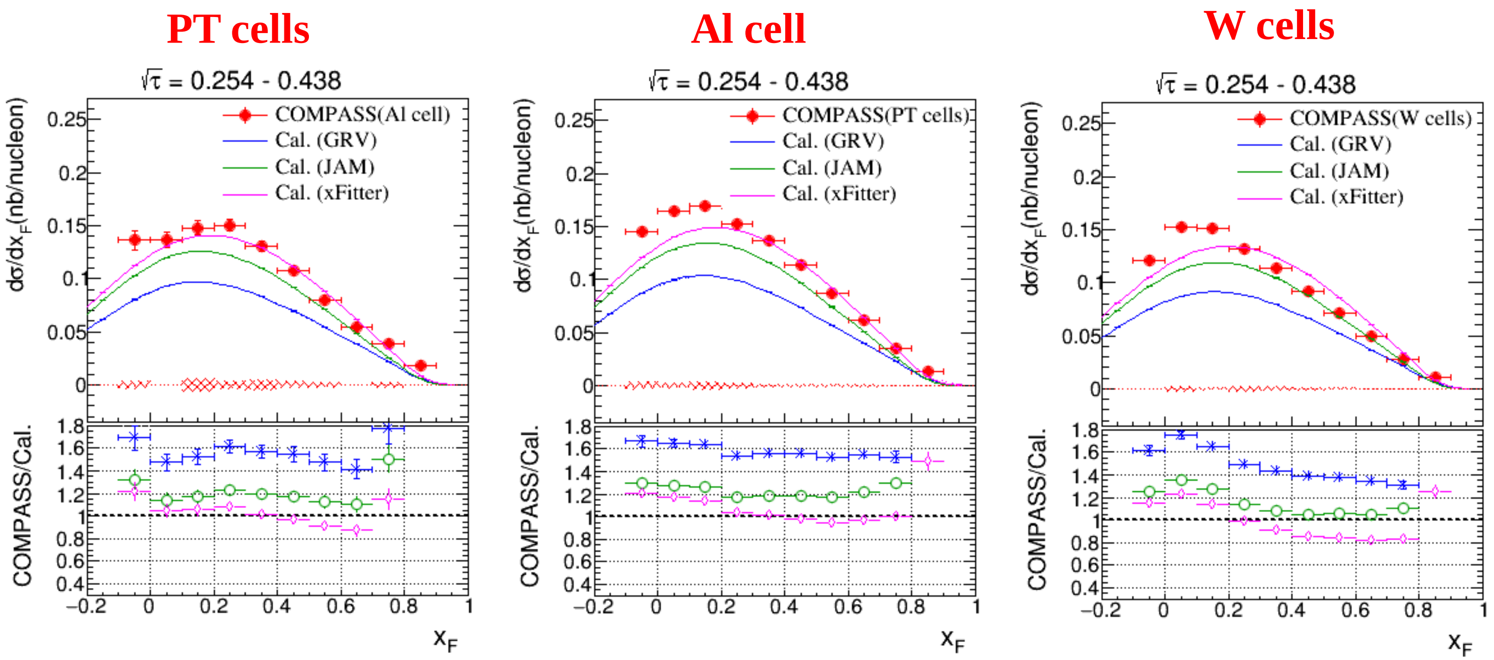

- **Theoretical calculation**

① **pQCD calculation in NLO** with nucleon PDF of CT14 and pion PDFs of **GRV, JAM, xFitter**.

② **Isospin average** is applied to nuclear target.

  a. W cells = (74p+110n)/(74+110) ~ 0.4p + 0.6n
  b. Al cell = (13p+ 13n)/(13+13) ~ 0.5p + 0.5n
  c. PT cells = NH_3+LHe ~ 0.6p + 0.4n

③ **No nuclear effect** included.

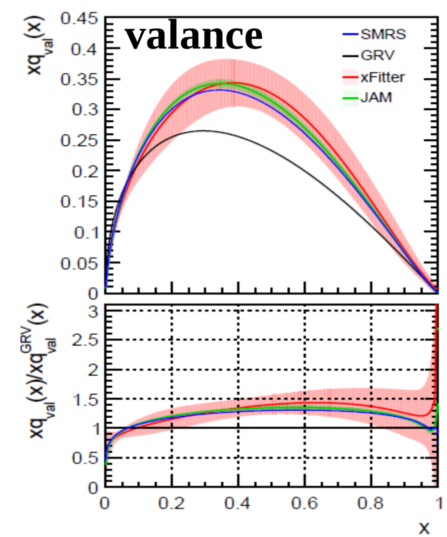

COMPASS results are in favor of JAM and xFitter have larger valence contribution compared to GRV.

Comparison with pQCD NLO Calculations

W cells

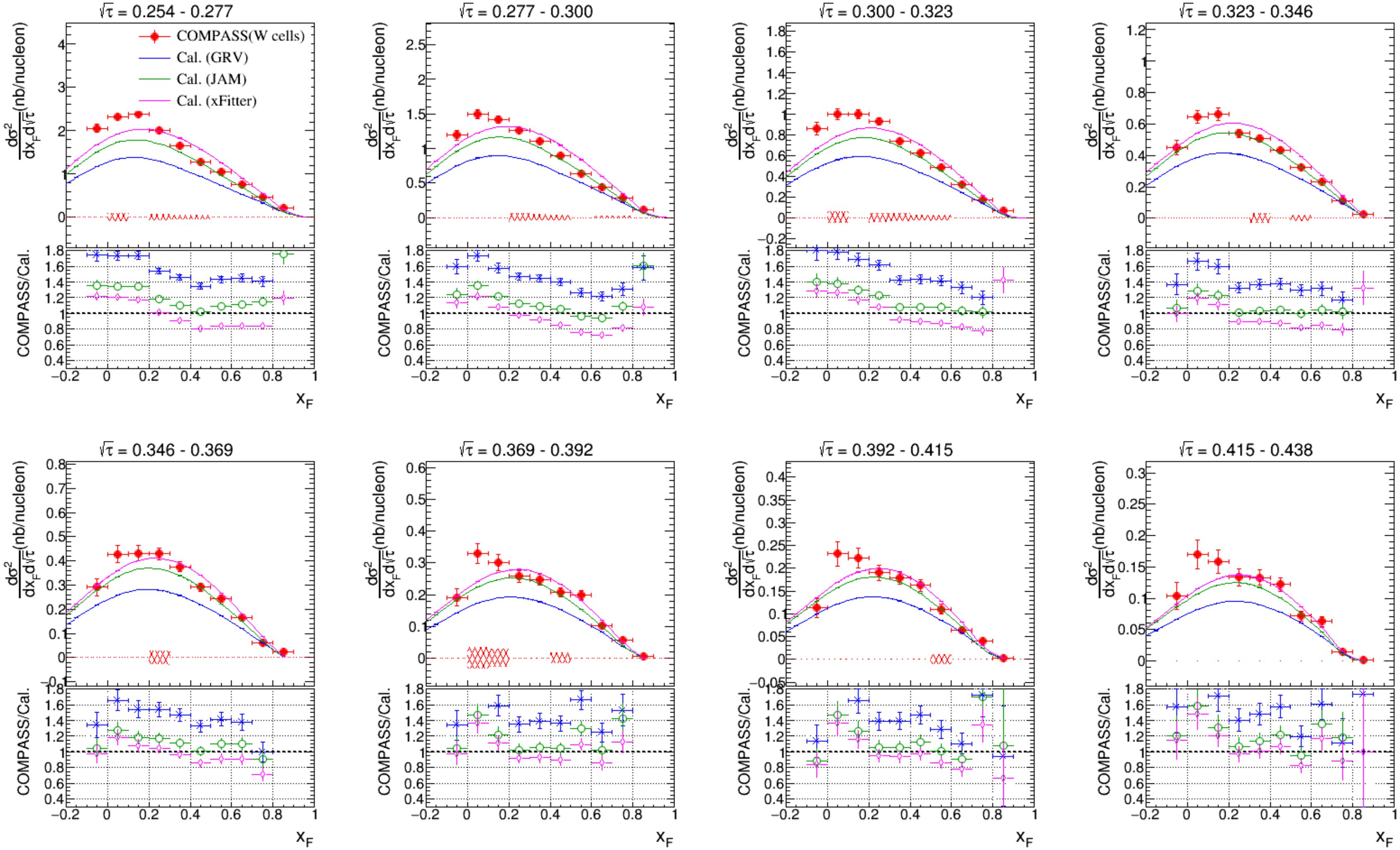

The same conclusion obtained when looking into different $\sqrt{\tau}$ region.

Comparison with pQCD NLO Calculations

PT cells

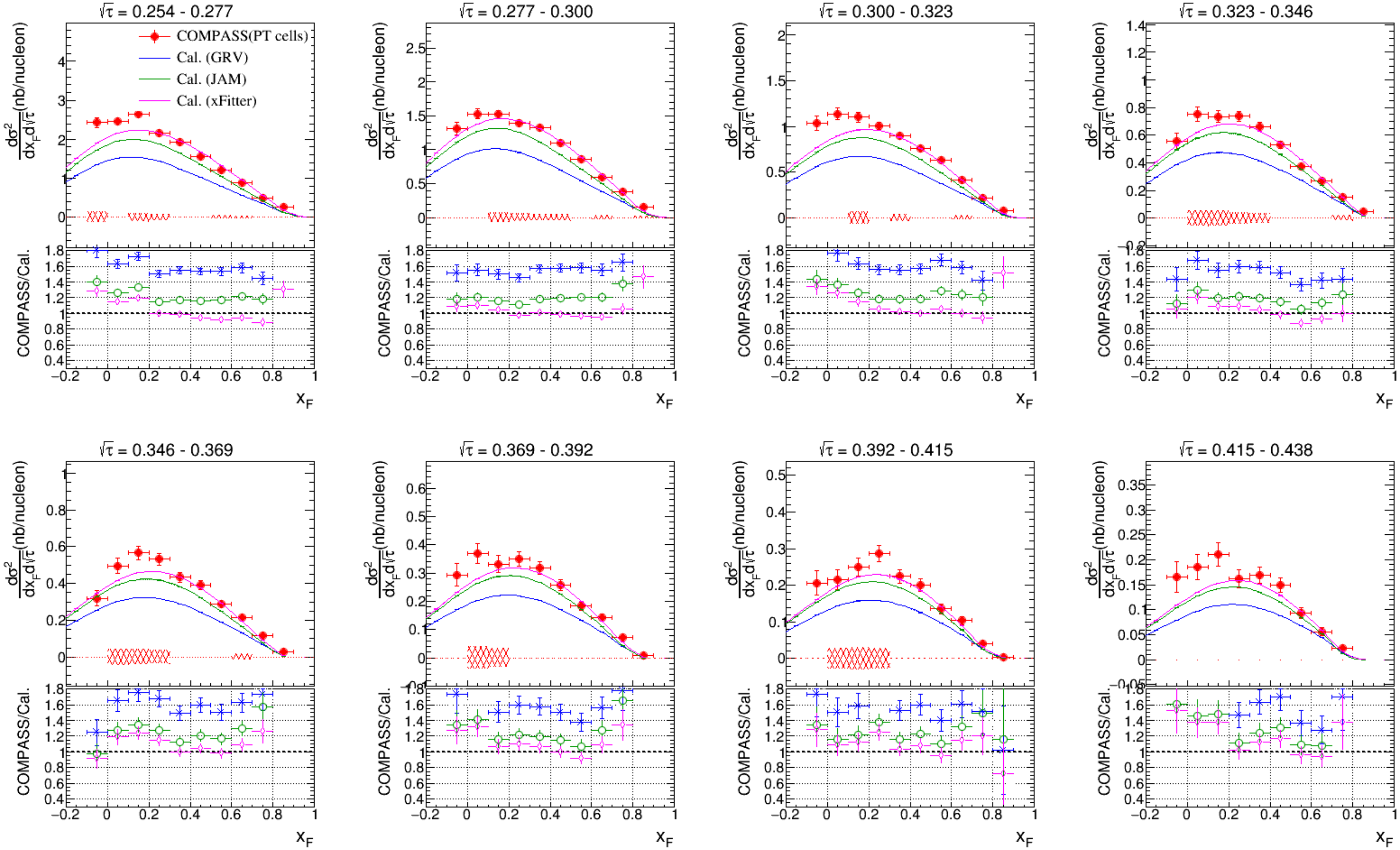

The same conclusion obtained when looking into different $\sqrt{\tau}$ region.

Comparison with pQCD NLO Calculations

Al cell

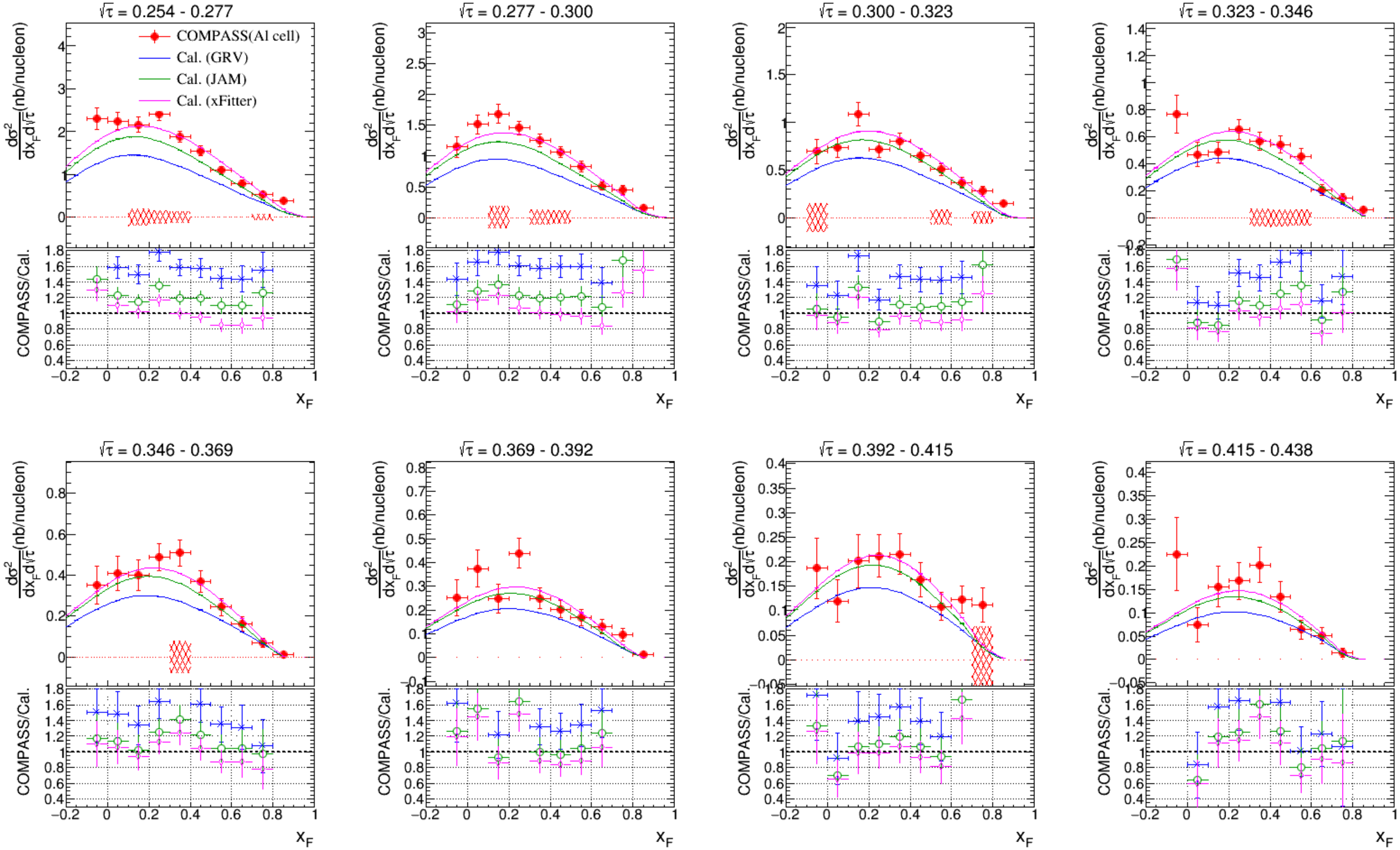

The same conclusion obtained when looking into different $\sqrt{\tau}$ region.

Nuclear Effect – Energy Lose

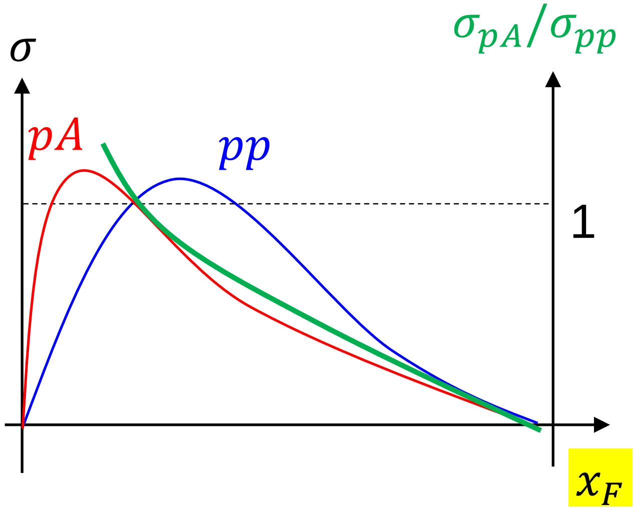

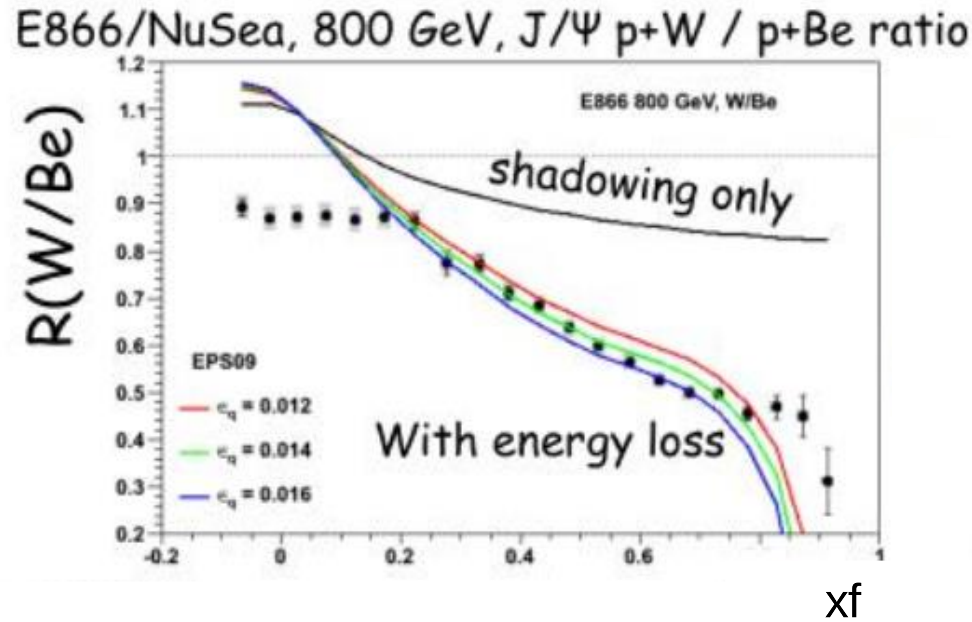

- Parton energy lose is caused by the gluon radiation of parton.
- **The stronger gluon radiation occurs inside heavier nuclear material**, therefore the mean xf distribution is smaller.
- Energy lose effect only occurs in the initial state of DY process, but occurs in both initial and final states of J/Psi process.

Nuclear Effect Observation w/ COMPASS Data

W cells / PT cells

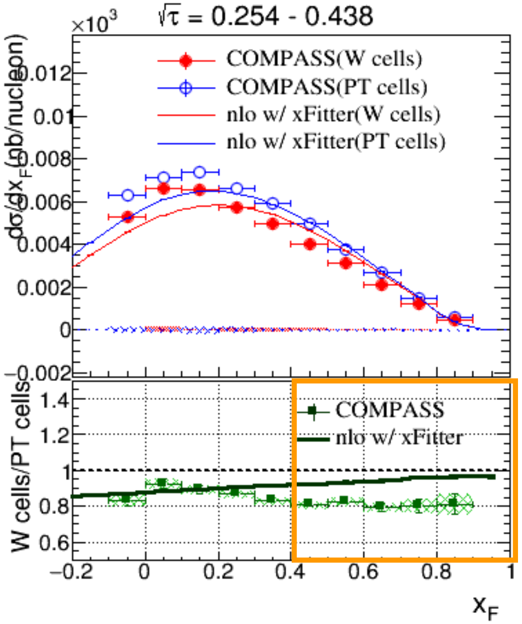

W cells/Al cell

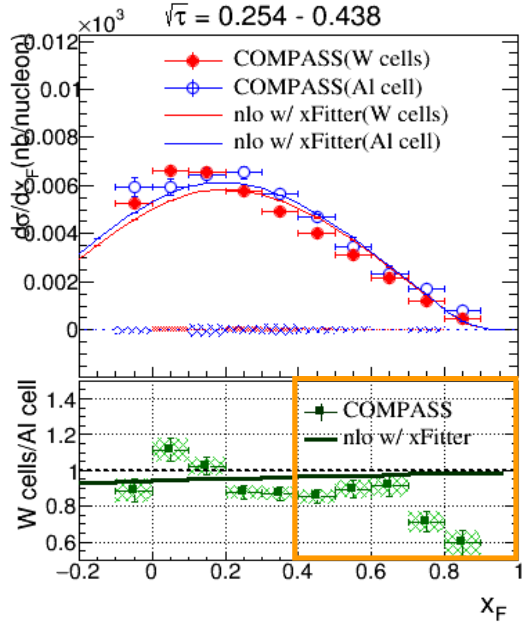

Al cell/PT cells

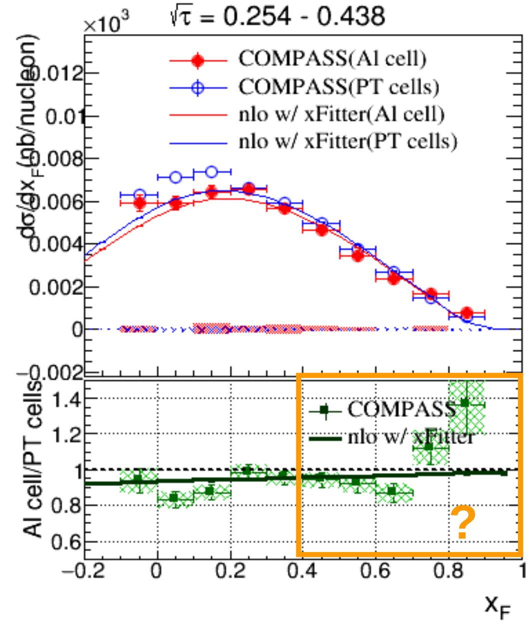

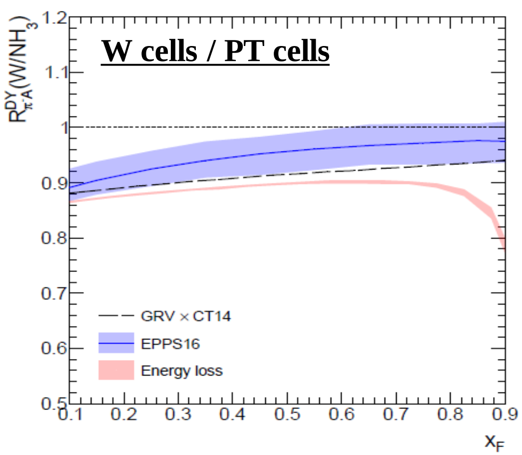

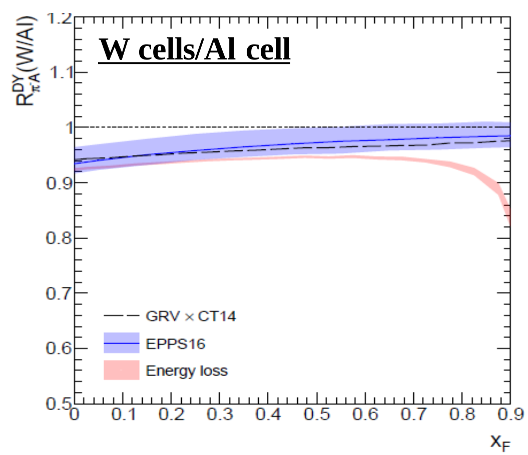

Charles-Joseph Naïm's phD thesis

Nuclear Effect Observation w/ COMPASS Data

W cells / Al cells

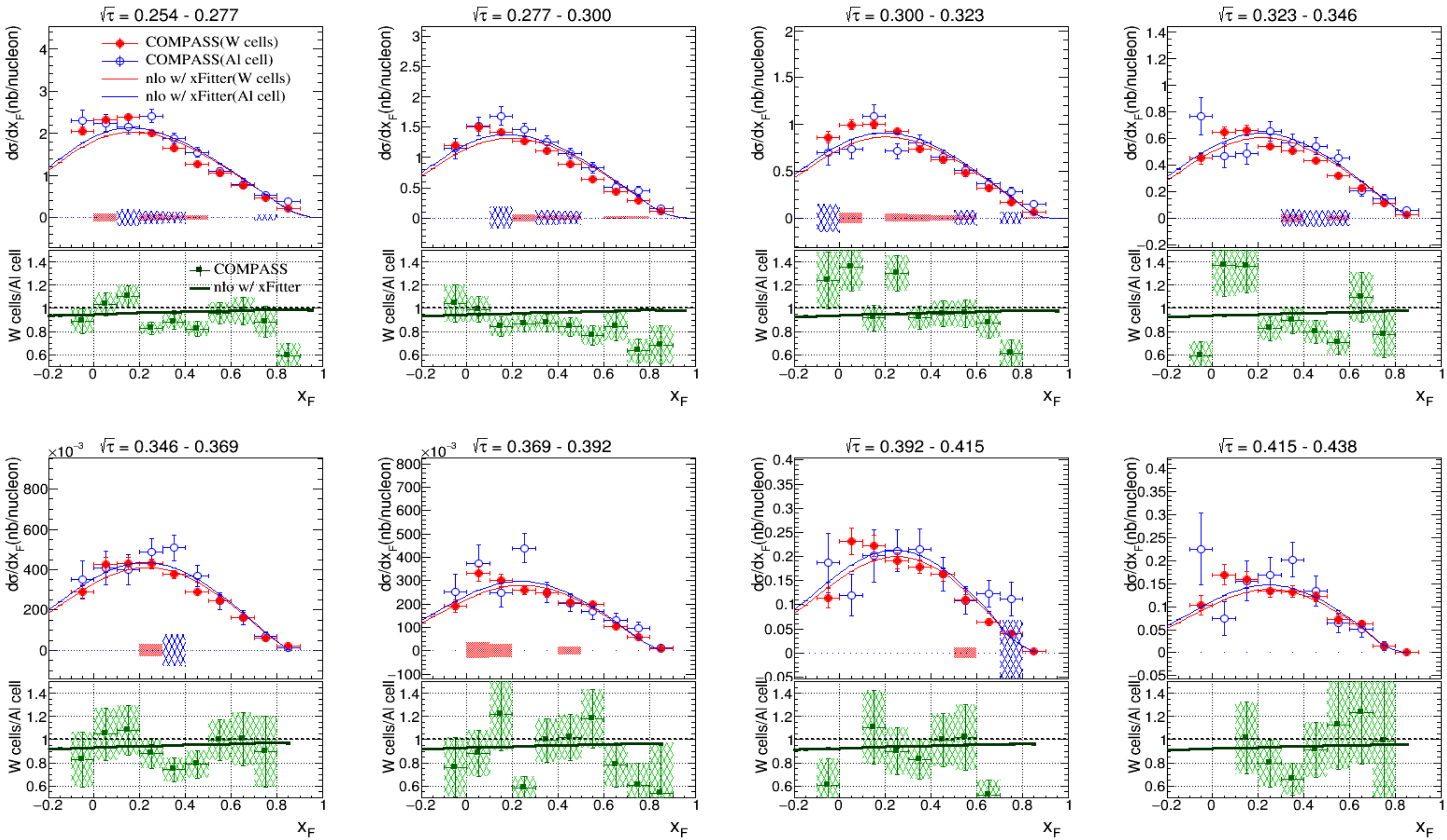

Nuclear Effect Observation w/ COMPASS Data

W cells / PT cells

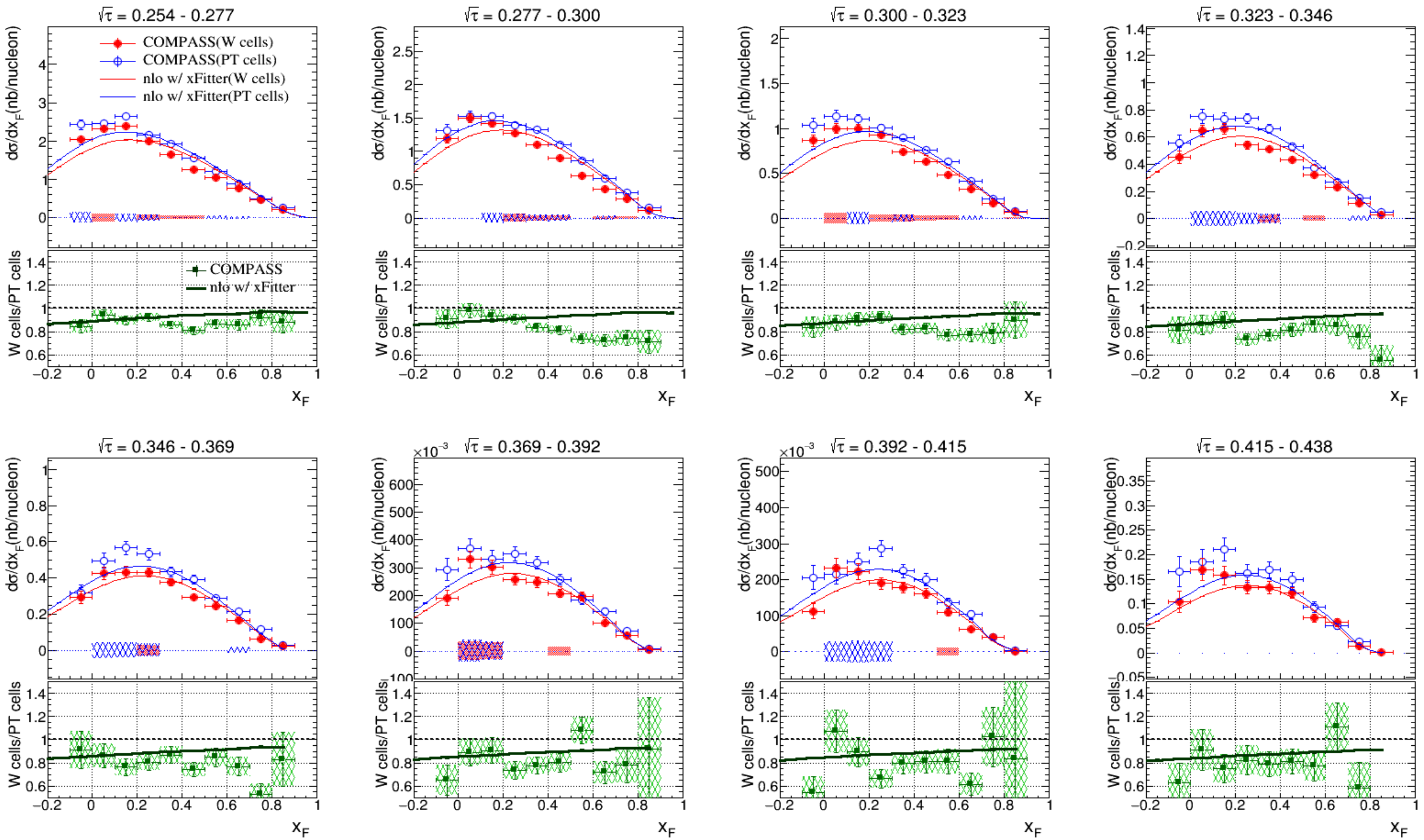

Nuclear Effect Observation w/ COMPASS Data

Al cells/PT cells

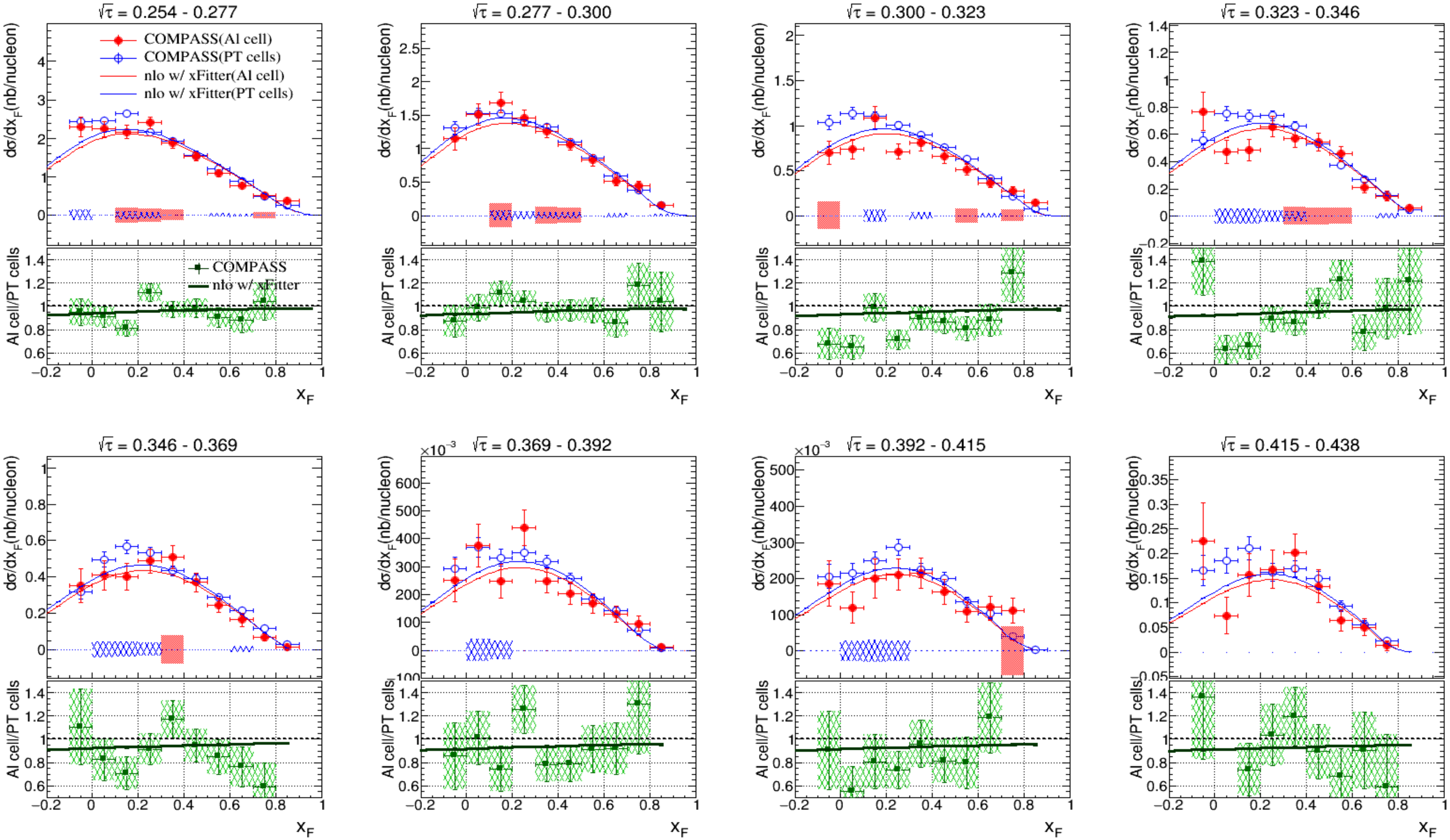

Drell-Yan Cross-Section in $d^2\sigma/dp_T\,dx_F$ and $d^2\sigma/dp_T\,d\sqrt{\tau}$

Pion-Induced Drell-Yan Process

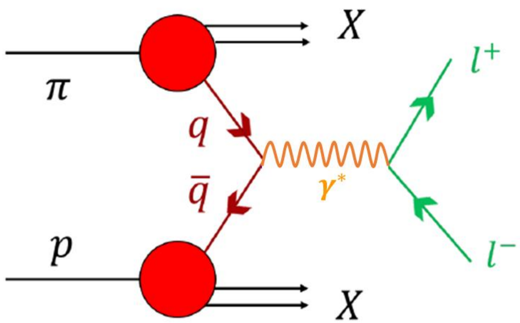

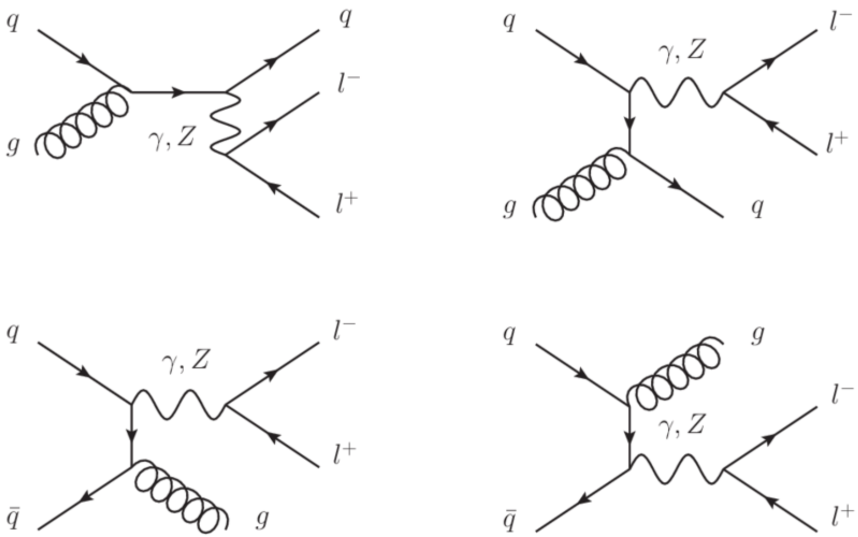

$LO \quad : \; q\bar{q} \to \gamma^* \to l^+l^-$

$NLO : \; q\bar{q}g \to \gamma^* \to l^+l^-g, \qquad qg \to \gamma^* \to l^+l^-q$

Journal of High Energy Physics
Article number: 90 (2019)

$$\frac{d^3\sigma}{dM_{ll}dx_F\mathbf{dp_T}} = \sigma_0 \sum_{f_\pi, f_p} H_{f\pi fp}(M_{ll},\mu) \int \frac{d^2\mathbf{b}}{4\pi} e^{i(\mathbf{b}\cdot\mathbf{p_T})} F_{h\pi\to f\pi}(x_\pi, \mathbf{b}; \mu, \zeta_1) F_{hp\to fp}(x_p, \mathbf{b}; \mu, \zeta_1)$$

TMD

- p_T specrum of **COMPASS data** is at the level of a few GeV which is in the range of the **soft gluon radiation** could **make contribution to the TMD of pion study**.
- p_T **broadening effect(nuclear effect)** can be studied by comparing the p_T spectrum between light and heavy targets. $< p_T >$ of heavy target is larger than the light target due to the multiple scattering of parton inside the nucleus.

W cells

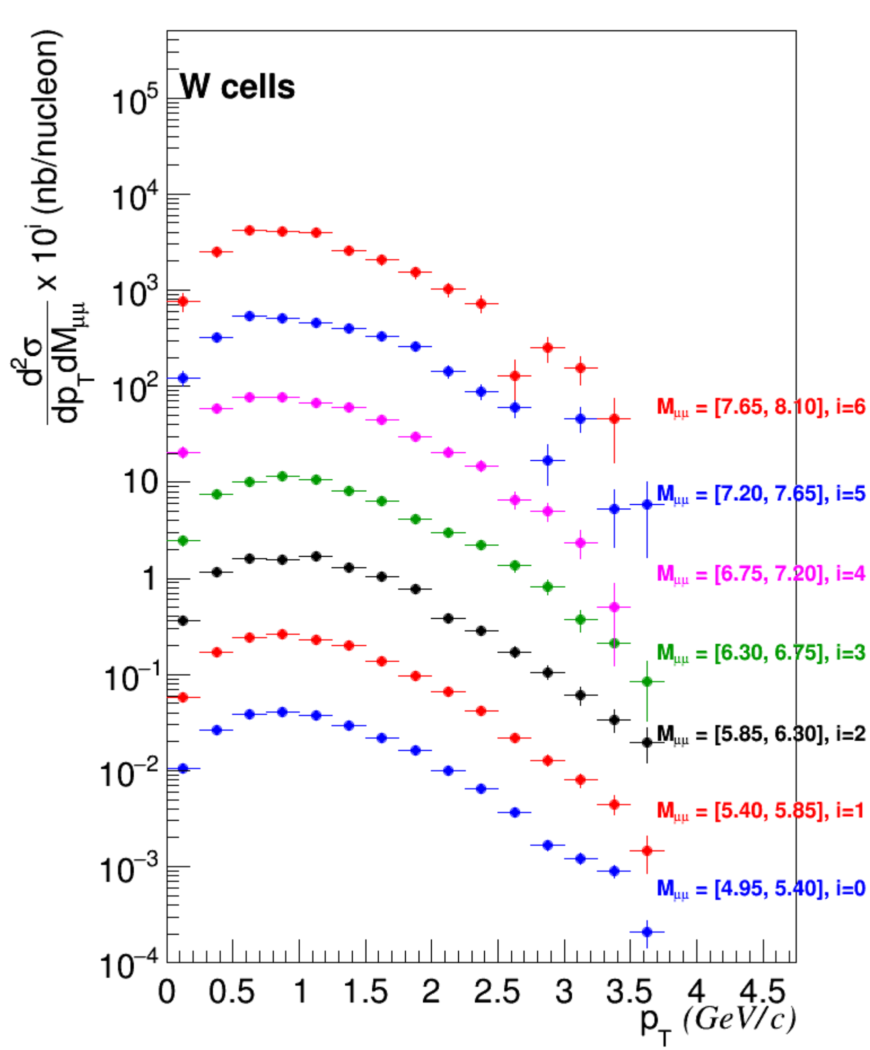
W cells
$\frac{d^2\sigma}{dp_T dM_{\mu\mu}} \times 10^i$ (nb/nucleon)
$M_{\mu\mu}$ = [7.65, 8.10], i=6
$M_{\mu\mu}$ = [7.20, 7.65], i=5
$M_{\mu\mu}$ = [6.75, 7.20], i=4
$M_{\mu\mu}$ = [6.30, 6.75], i=3
$M_{\mu\mu}$ = [5.85, 6.30], i=2
$M_{\mu\mu}$ = [5.40, 5.85], i=1
$M_{\mu\mu}$ = [4.95, 5.40], i=0
p_T (GeV/c)

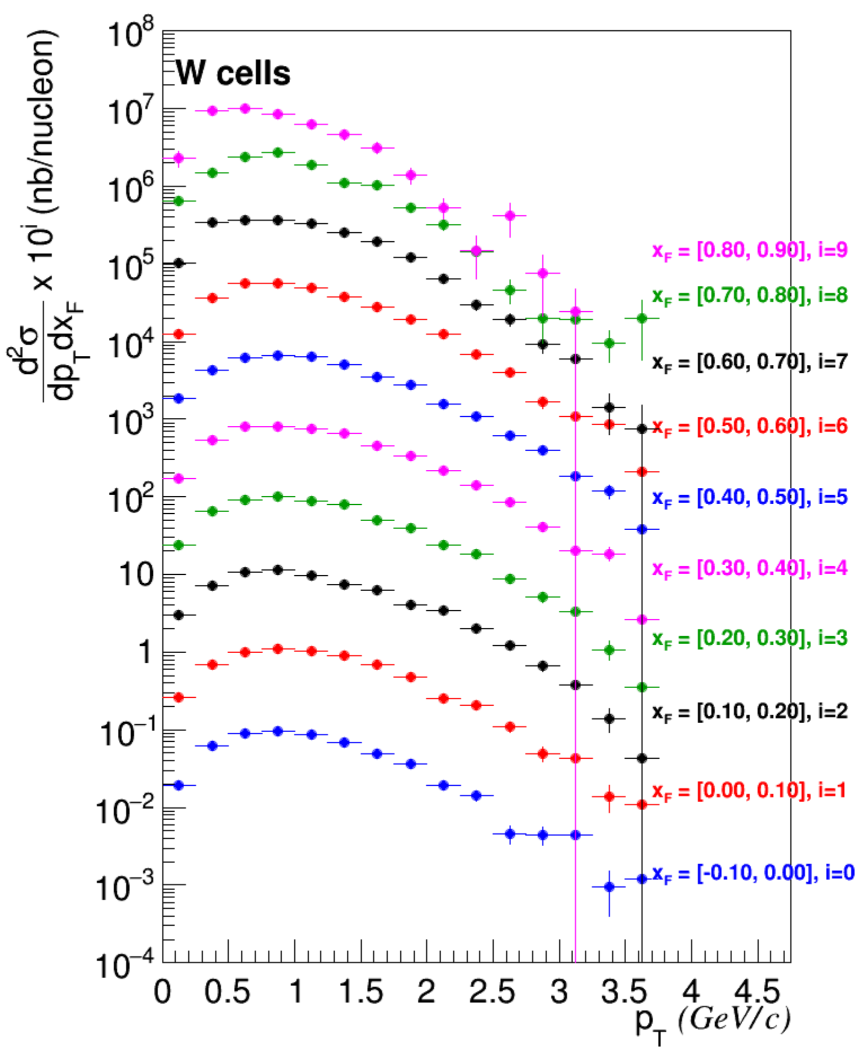
W cells
$\frac{d^2\sigma}{dp_T dx_F} \times 10^i$ (nb/nucleon)
x_F = [0.80, 0.90], i=9
x_F = [0.70, 0.80], i=8
x_F = [0.60, 0.70], i=7
x_F = [0.50, 0.60], i=6
x_F = [0.40, 0.50], i=5
x_F = [0.30, 0.40], i=4
x_F = [0.20, 0.30], i=3
x_F = [0.10, 0.20], i=2
x_F = [0.00, 0.10], i=1
x_F = [-0.10, 0.00], i=0
p_T (GeV/c)

PT cells

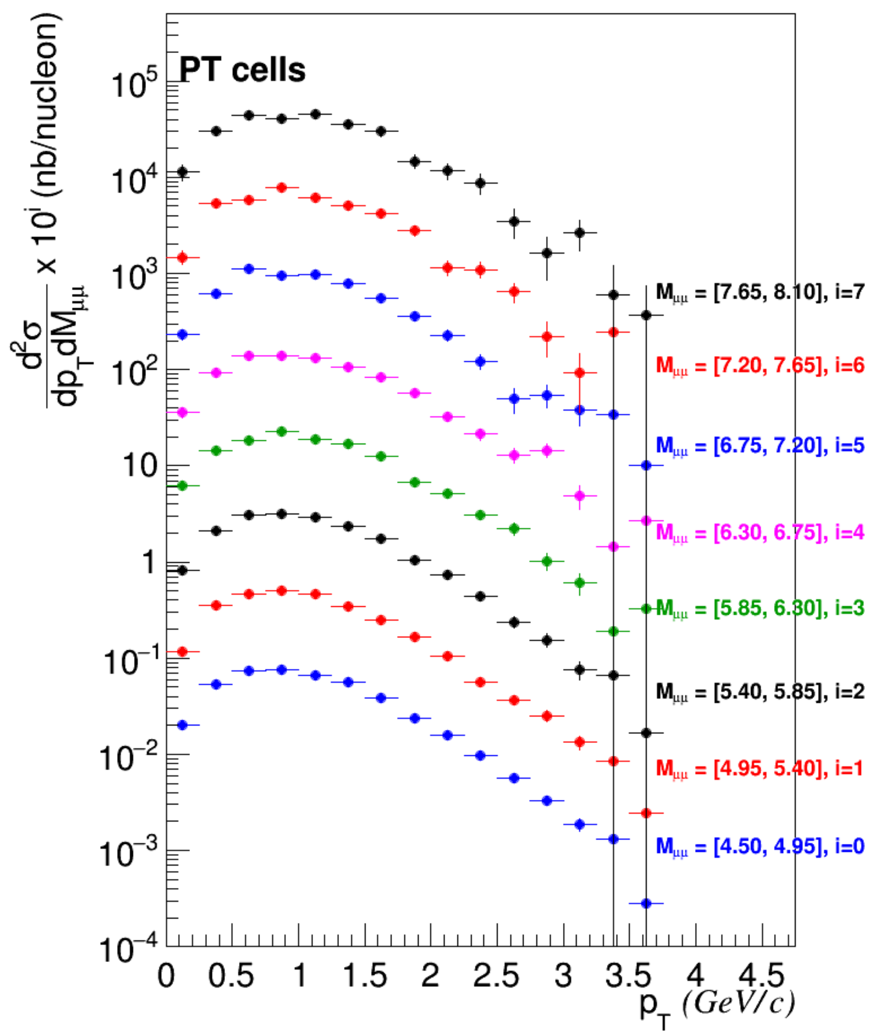

PT cells
$\frac{d^2\sigma}{dp_T dM_{\mu\mu}} \times 10^i$ (nb/nucleon)
$M_{\mu\mu}$ = [7.65, 8.10], i=7
$M_{\mu\mu}$ = [7.20, 7.65], i=6
$M_{\mu\mu}$ = [6.75, 7.20], i=5
$M_{\mu\mu}$ = [6.30, 6.75], i=4
$M_{\mu\mu}$ = [5.85, 6.30], i=3
$M_{\mu\mu}$ = [5.40, 5.85], i=2
$M_{\mu\mu}$ = [4.95, 5.40], i=1
$M_{\mu\mu}$ = [4.50, 4.95], i=0
p_T (GeV/c)

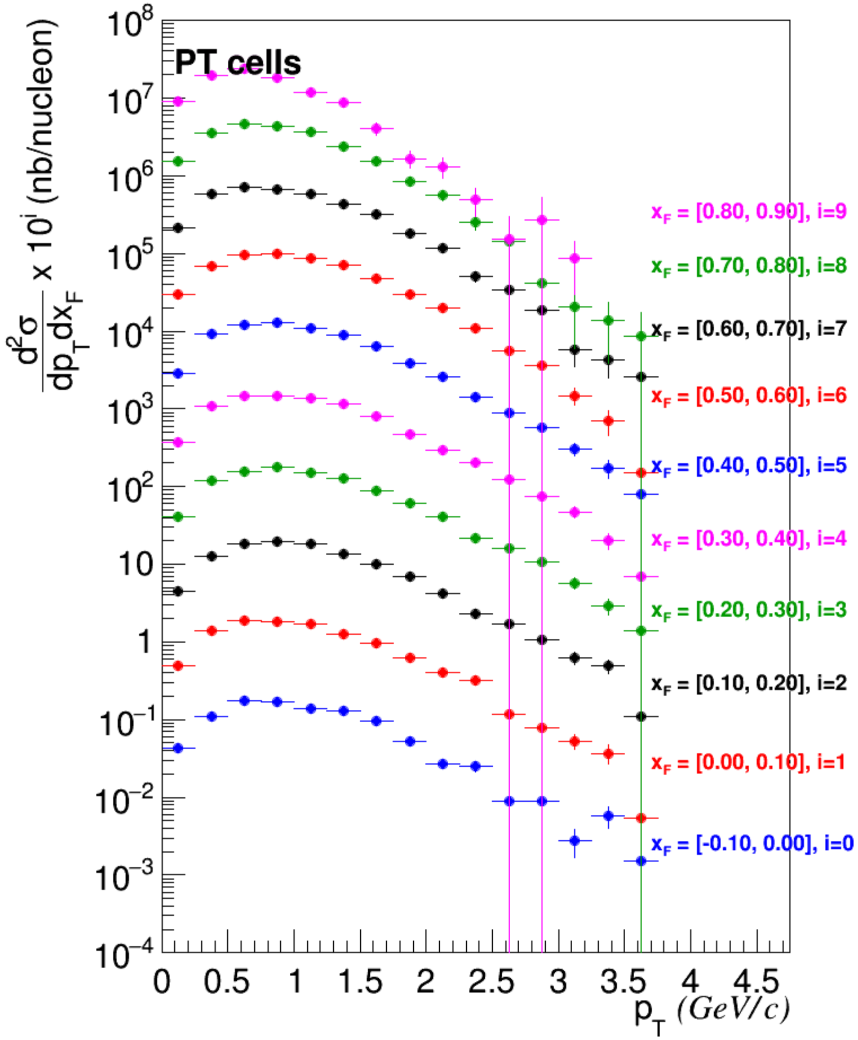

PT cells
$\frac{d^2\sigma}{dp_T dx_F} \times 10^i$ (nb/nucleon)
x_F = [0.80, 0.90], i=9
x_F = [0.70, 0.80], i=8
x_F = [0.60, 0.70], i=7
x_F = [0.50, 0.60], i=6
x_F = [0.40, 0.50], i=5
x_F = [0.30, 0.40], i=4
x_F = [0.20, 0.30], i=3
x_F = [0.10, 0.20], i=2
x_F = [0.00, 0.10], i=1
x_F = [-0.10, 0.00], i=0
p_T (GeV/c)

Al cell

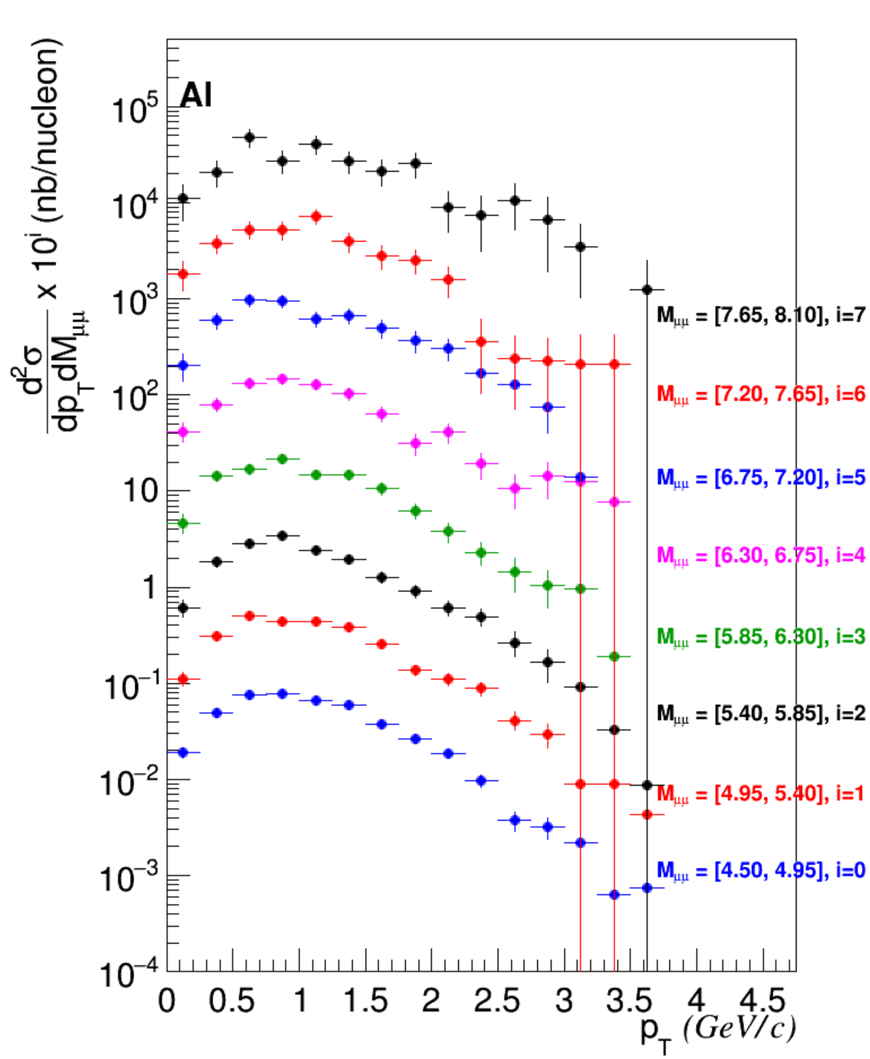

Al
$\frac{d^2\sigma}{dp_T dM_{\mu\mu}} \times 10^i$ (nb/nucleon)
p_T (GeV/c)
$M_{\mu\mu}$ = [7.65, 8.10], i=7
$M_{\mu\mu}$ = [7.20, 7.65], i=6
$M_{\mu\mu}$ = [6.75, 7.20], i=5
$M_{\mu\mu}$ = [6.30, 6.75], i=4
$M_{\mu\mu}$ = [5.85, 6.30], i=3
$M_{\mu\mu}$ = [5.40, 5.85], i=2
$M_{\mu\mu}$ = [4.95, 5.40], i=1
$M_{\mu\mu}$ = [4.50, 4.95], i=0

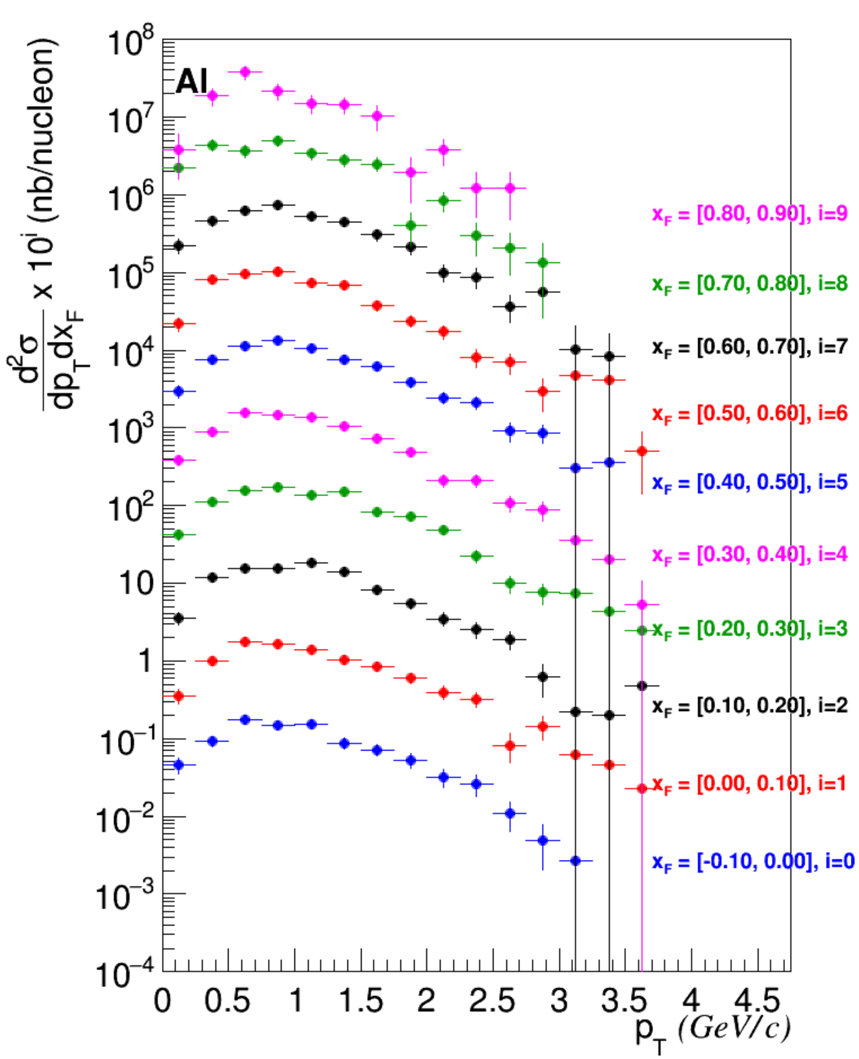

Al
$\frac{d^2\sigma}{dp_T dx_F} \times 10^i$ (nb/nucleon)
p_T (GeV/c)
x_F = [0.80, 0.90], i=9
x_F = [0.70, 0.80], i=8
x_F = [0.60, 0.70], i=7
x_F = [0.50, 0.60], i=6
x_F = [0.40, 0.50], i=5
x_F = [0.30, 0.40], i=4
x_F = [0.20, 0.30], i=3
x_F = [0.10, 0.20], i=2
x_F = [0.00, 0.10], i=1
x_F = [-0.10, 0.00], i=0

$< p_T^2 >$ Spectrum

$< p_T^2 >$ in different x_F bins

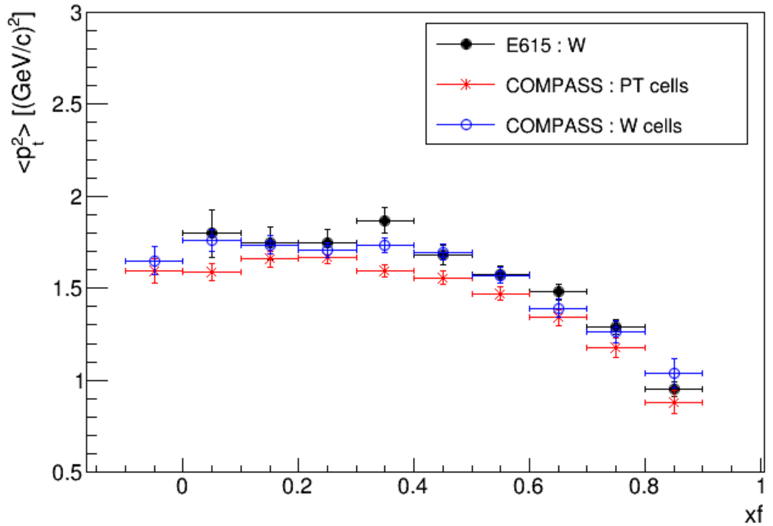

$< p_T^2 >$ in different $\sqrt{\tau}$ bins

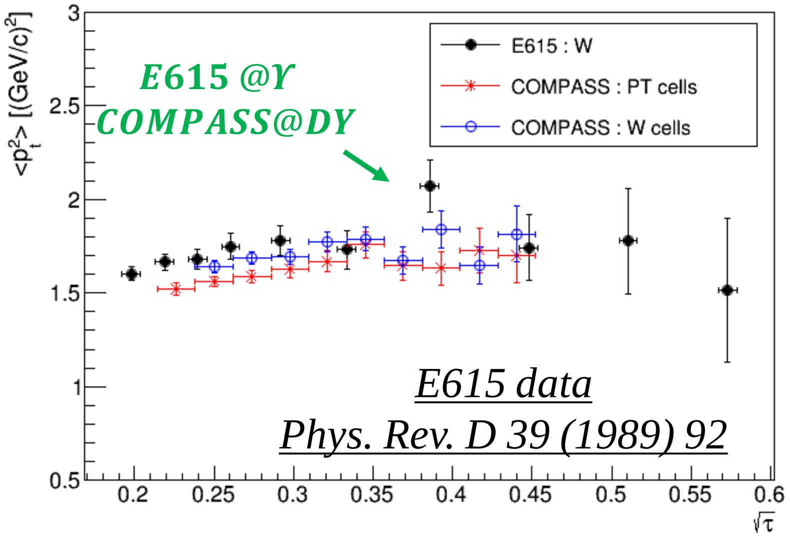

Bin summation method

$$< p_T^2 > = \frac{\sum_{bin=1}^{N} p_T^2 \frac{d\sigma}{dp_T} dp_T(i)}{\sum_{bin=1}^{N} \frac{d\sigma}{dp_T} dp_T(i)}$$

- The trends of $< p_T^2 >$ measured by COMPASS is consistent with E615. $< p_T^2 >$ decreases with the increase of x_F and increases with $M_{\mu\mu}$.
- The **nuclear effect, p_T broadening effect,** is validate : The larger $< p_T^2 >$ for heavier target due to the **multiple scattering of parton inside nucleon target.**

Systematics Uncertainty of Triggers

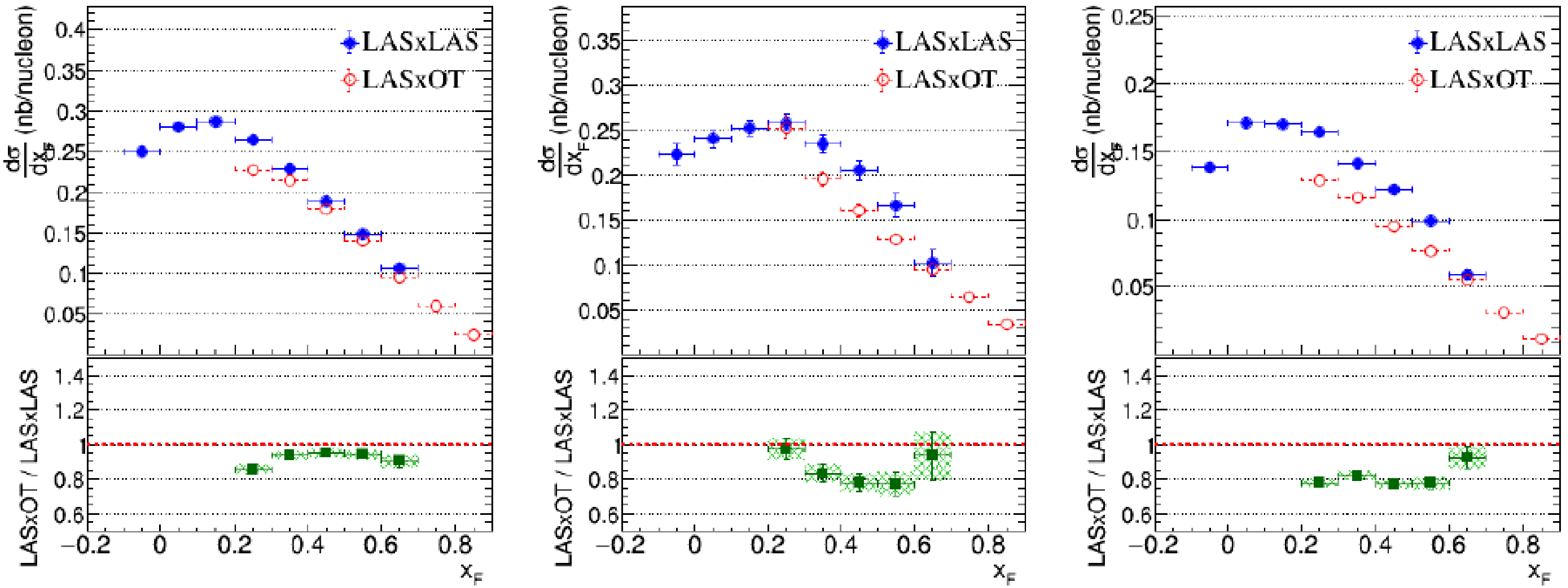

(a) *PT cells* (b) *Al cell* (c) *W cells*

Main contribution to the systematics, up to 20%.

Summary and Outlook

- The pion-induced Drell-Yan data is one of the main resource for the global fit of pion PDF and TMD. **The measurement of Drell-Yan cross section is performed with COMPASS 2018 data from $\pi^- N$ scattering with 190GeV π^- beam and 3 kinds of targets, ammonia polarized target, alumina, and tungsten.**

- The pion-induced Drell-Yan cross section measured by COMPASS shows a **reasonable agreement with both pQCD calculation in NLO and the past results given by NA10 and E615 experiments**. The nuclear effects, pt broadening and the energy loss effect are also observed by comparing the DY cross section between different targets.

- We are now still struggling with the **20% systematics uncertainty from the trigger dependence** of Drell-Yan cross section (Systematic from E165 ~15% and NA10 ~5%). If this problem can be solved, COMPASS data would be used as a new input of **the global fit of pion PDF and TMD, and the study of nuclear effect.**

Back Up

Multi-Dimensional Hadron Structure

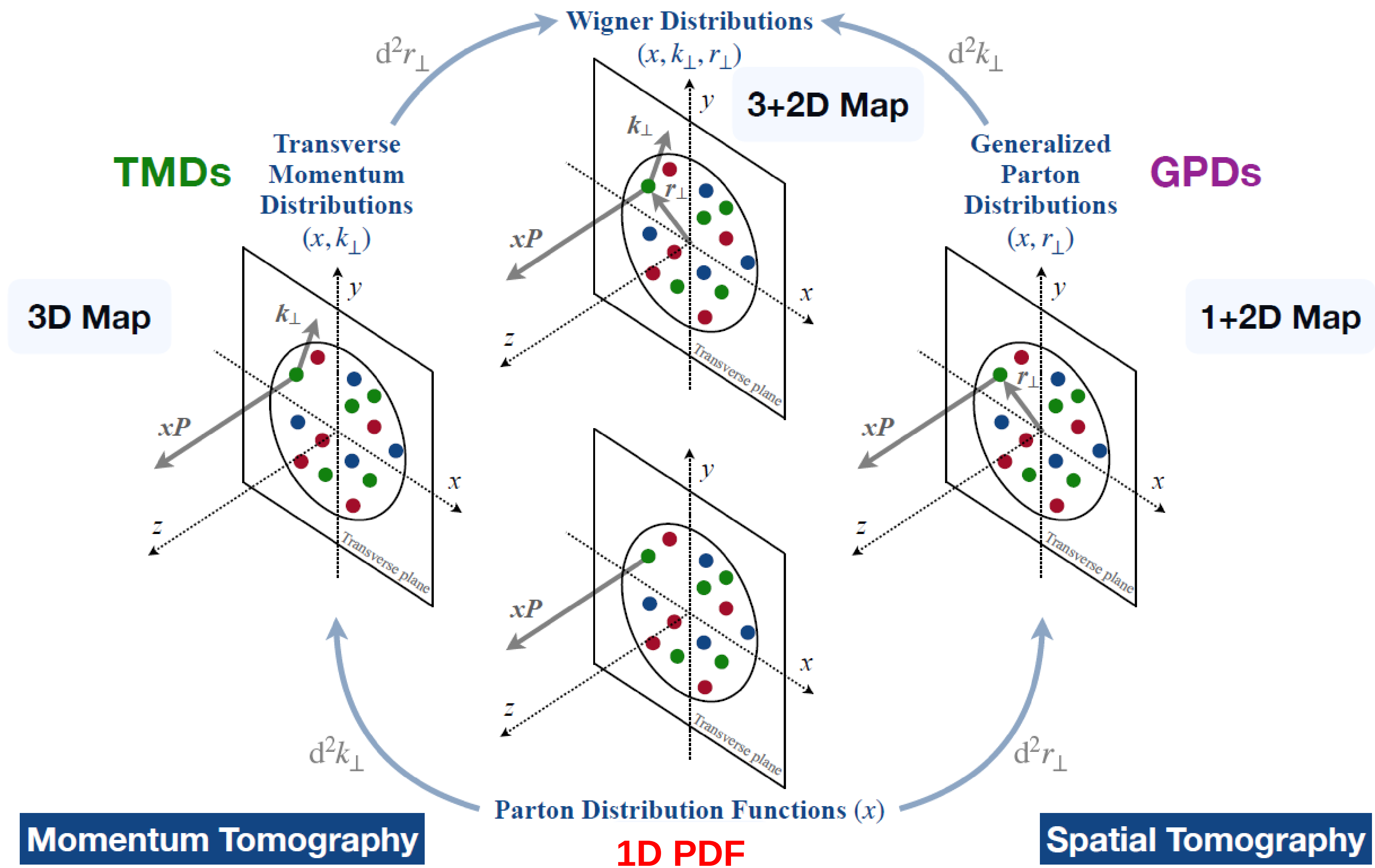

Proton PDF

Deep Inelastic Scattering (DIS)

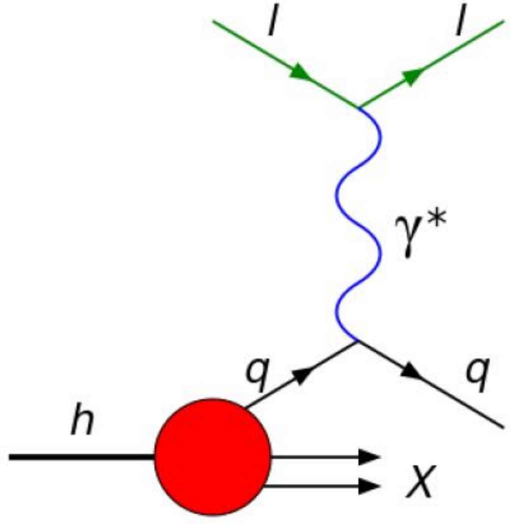

Proton PDF from NNPDF set

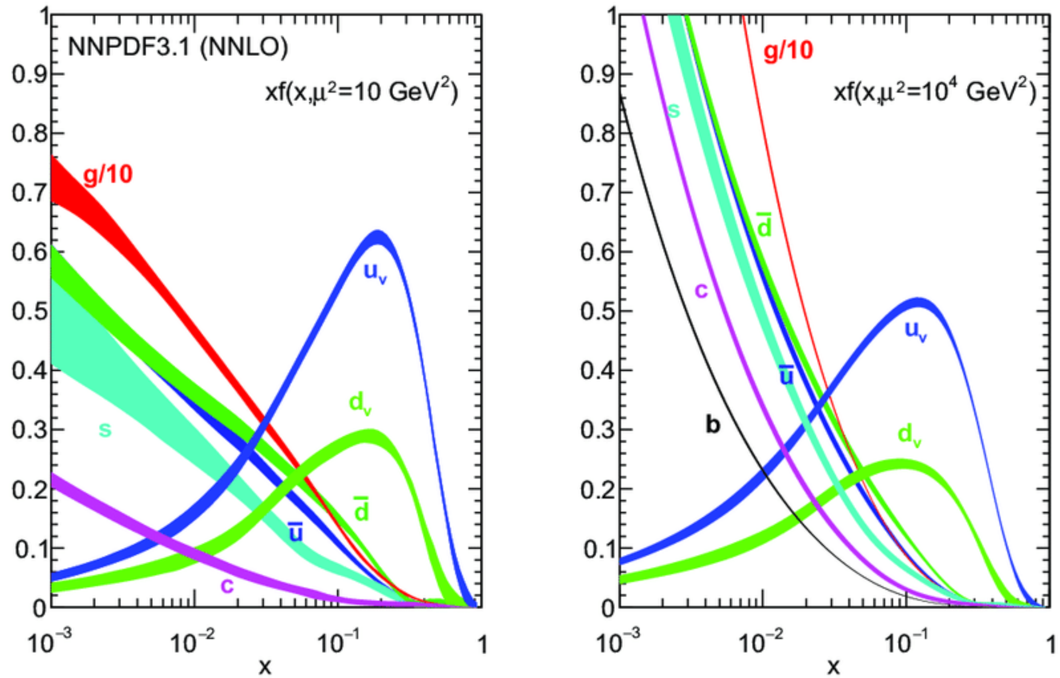

- SLAC-MIT group (Bloom et al.) in 1969 performed DIS ep scattering with around 20 GeV electron beams. The proton structure was first studied. Until now, the proton PDF is well defined due to the high statistic DIS data worldwide.

- However, the pion structure is not investigated as much as proton due to the **lack of pion target** to perform DIS experiment. **Pion PDFs are extracted with limited data from the experiments with pion-nucleon scattering.**

Beam Flux

Random Trigger Method

$$\mathcal{F}_{RT} = \frac{\sum N_{beam}^{RT}}{\sum N_{RT} \times \Delta t_{window}^{RT}}$$

A fixed time window(7ns) open for each arriving random trigger and the number of beam is counted within this time window. The averaged beam flux per second is given by dividing the accumulated number of beam to the accumulated time window.

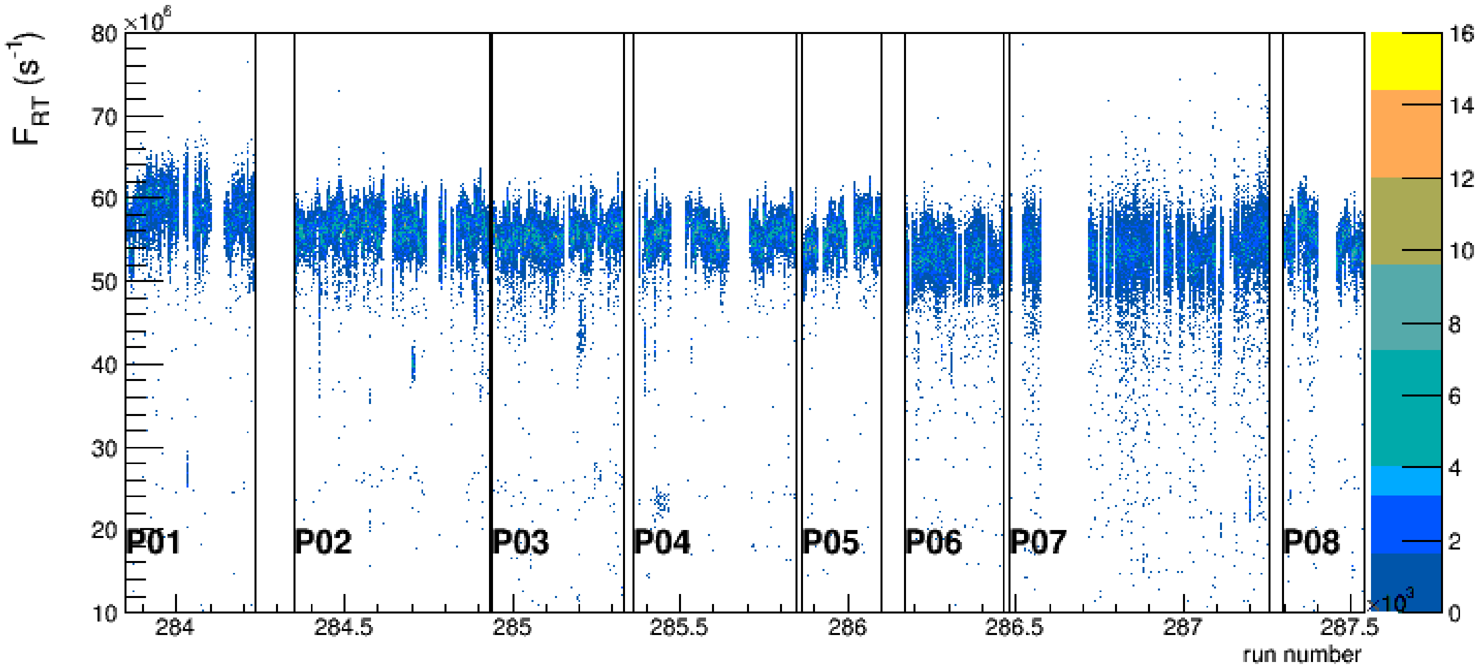

The beam flux in 2018 Drell-Yan data taking is around $60 \times 10^6 (s^{-1})$.

Efficiency of DAQ, ε_{DAQ}

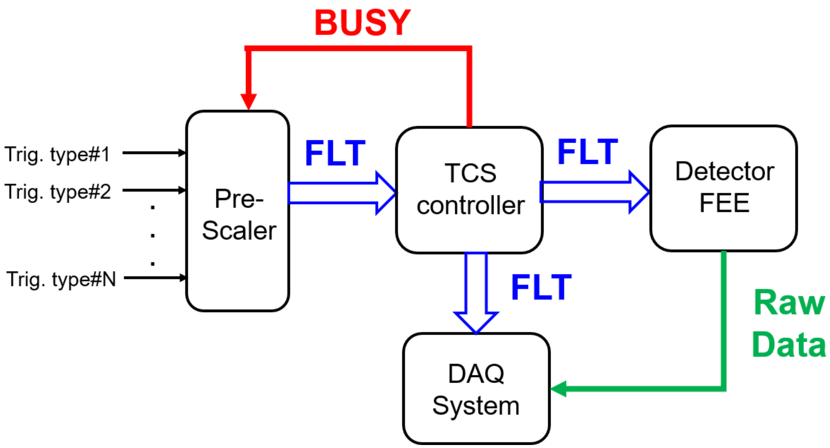

Once Trigger-Clock System(TCS) detects the limitation of the trigger rates DAQ system can handle. TCS sends a BUSY signal to prescalar to stop it sending more first-level trigger (FLT) for a short time. This causes the lose of FLT. The limitation of COMPASS DAQ in DY run is around 30kHz.

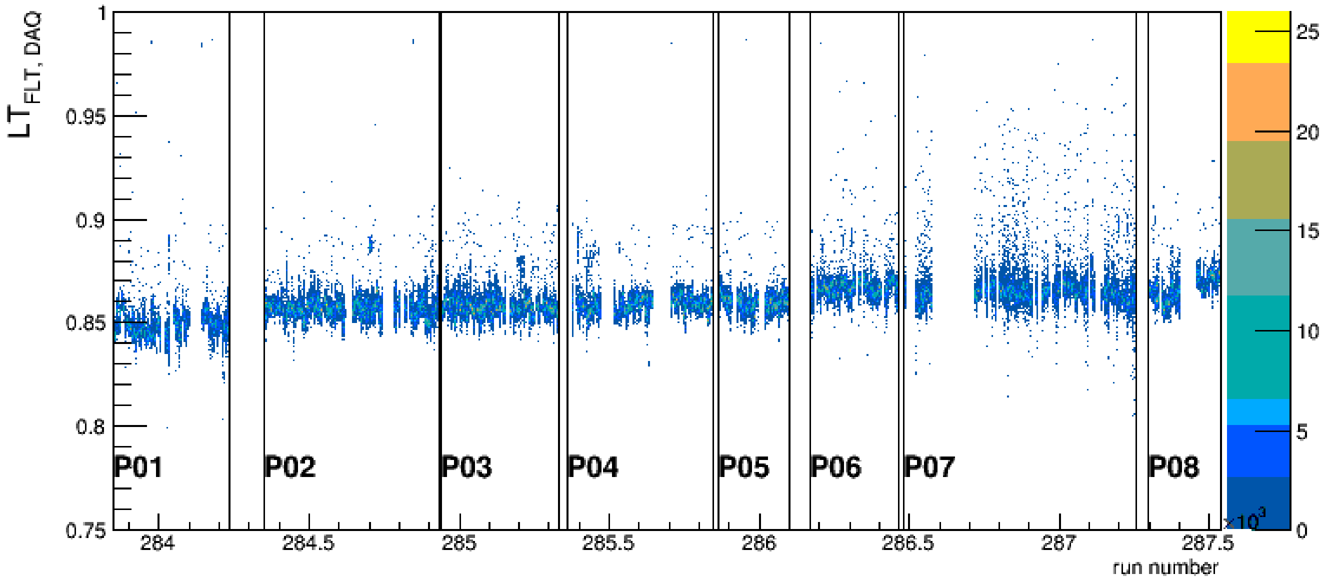

Efficiency of DAQ is around 85%.

Efficiency of Beam VETO, ε_{VETO}

Beam VETO trigger inhibits the muon tracks which do not interact with the targets. It is anti-coincident with the single triggers, LAS and OT. Beam VETO also cause the lose of true muon triggers because of the time window opened of VETO signal.

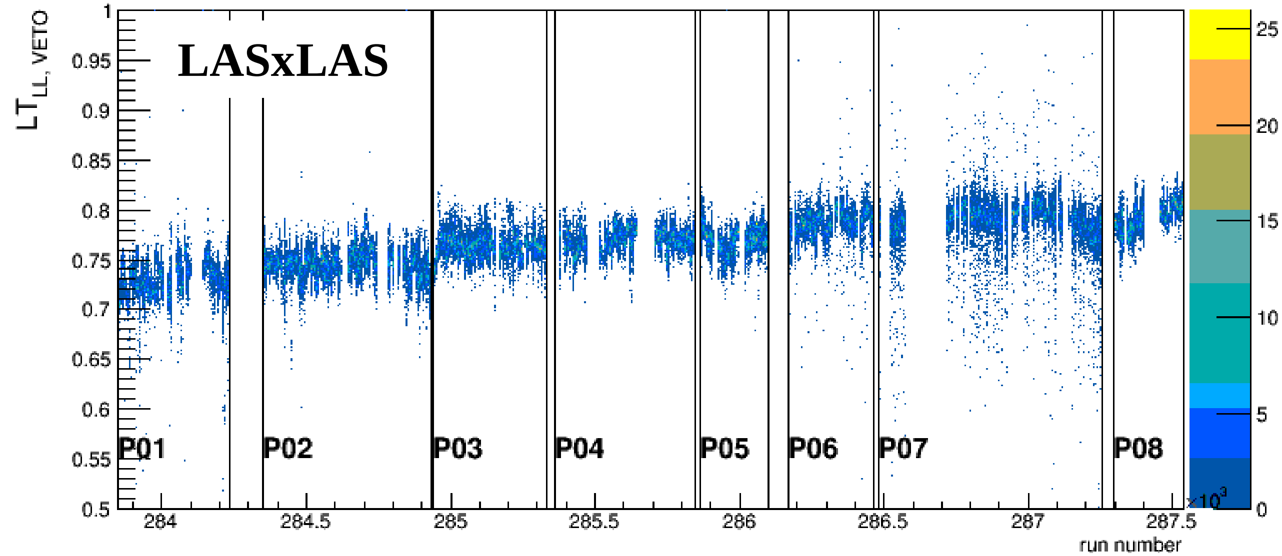

Efficiency of VETO

75% for LASxLAS
65% for LASxOT.

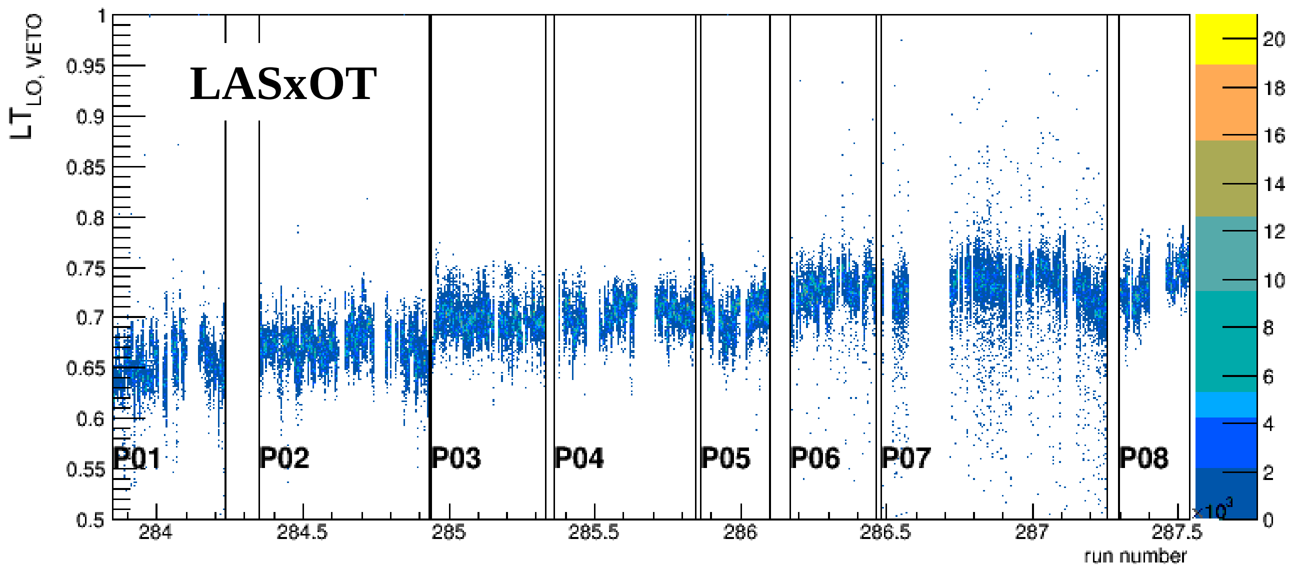

Efficiency of Acceptance

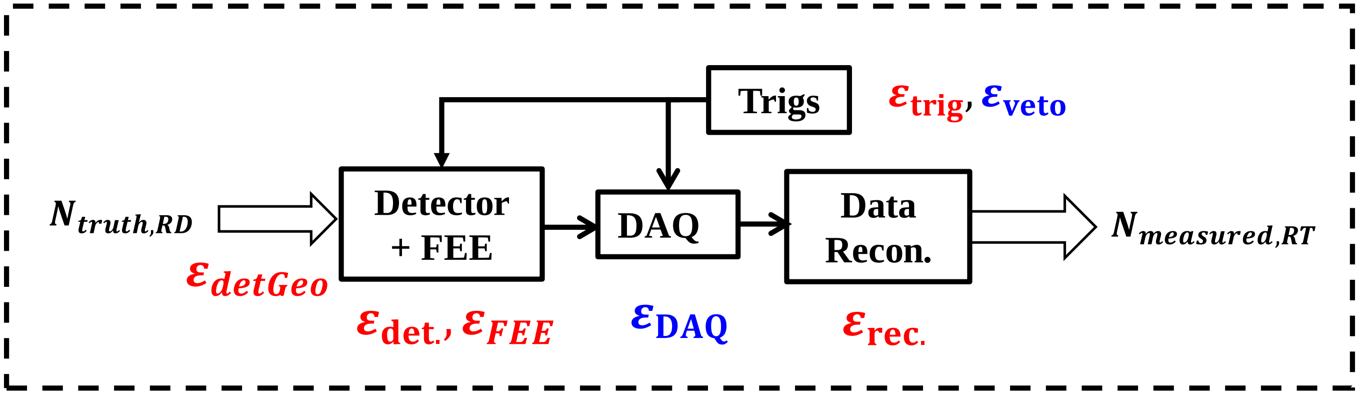

$\varepsilon_{acc} = \varepsilon_{detGeo} \times \varepsilon_{\mathrm{det.}} \times \varepsilon_{FEE} \times \varepsilon_{\mathrm{trig}} \times \varepsilon_{\mathrm{rec.}}$ simulated by MC

- **Materials require for MC**

(1) **Drell-Yan process event setting in Pythia8**
(2) **Information of beam :** profile, beam intensity, and pileup,
(3) **Efficiency of trigger :** geometric descriptions, detector efficiency, trigger matrix efficiency.
(4) **Efficiency of detectors :** geometry descriptions, detector+FEE efficiency.

MC simulates most of the efficiencies. Among them, trigger efficiency is the one affects the most since it varied more than 20% along the time due to the instable hodoscope condition.

Systematics Uncertainty from Luminosity and Lifetime

Table 24: *The overall systematic uncertainties of the Drell-Yan cross section contributed by the luminosity and the lifetime estimation.*

	PT cells	Al cell	W cells
Beam Flux	1 %	1%	1%
DAQ Lifetime	1%	1%	1%
VETO Lifetime	1%	1%	1%
Beam Composition	1%	1%	1%
Target Composition	2%	-	-

Negligible

Systematics Uncertainty from Reinteraction

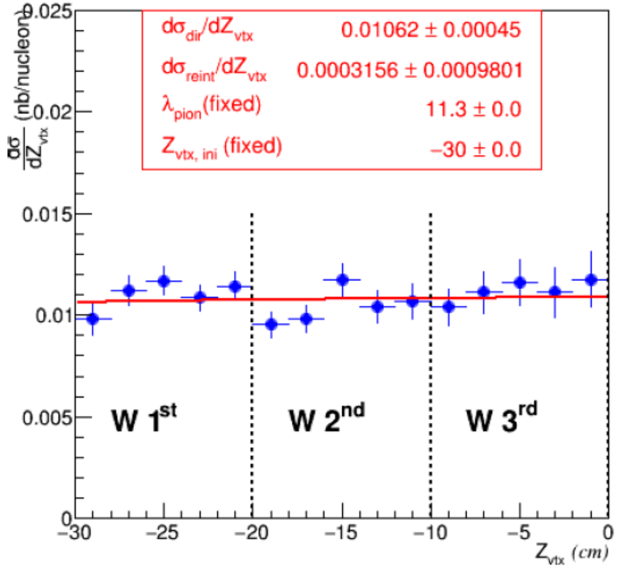

Negligible

The re-interaction effect is defined as the Drell-Yan cross section contributed by the secondary pions scatter the target. The secondary pion is produced from the hadronization of the primary pion beam and target interaction. The re-interaction effect is not simulated in the MC simulation, therefore it has to be corrected. The re-interaction effect increases with longer and heavier targets. In this analysis, only W cells requires the correction of re-interaction effect. In Ref. [92], the formulation of the re-interaction effect is defined as follows :

$$\sigma_{measure} = \sigma_{direct} + \sigma_{reint}\ [1 - \frac{L/\lambda_{int,pion}}{exp(L/\lambda_{int,pion}) - 1}]$$

where L is the physical length of target, $\lambda_{int,pion}$ is the pion interaction length in the unit of cm, $\sigma_{measure}$ is the measured cross section, σ_{direct} is the true cross section, σ_{reint} is the re-interacted cross-section.

Systematics Uncertainty of Periods

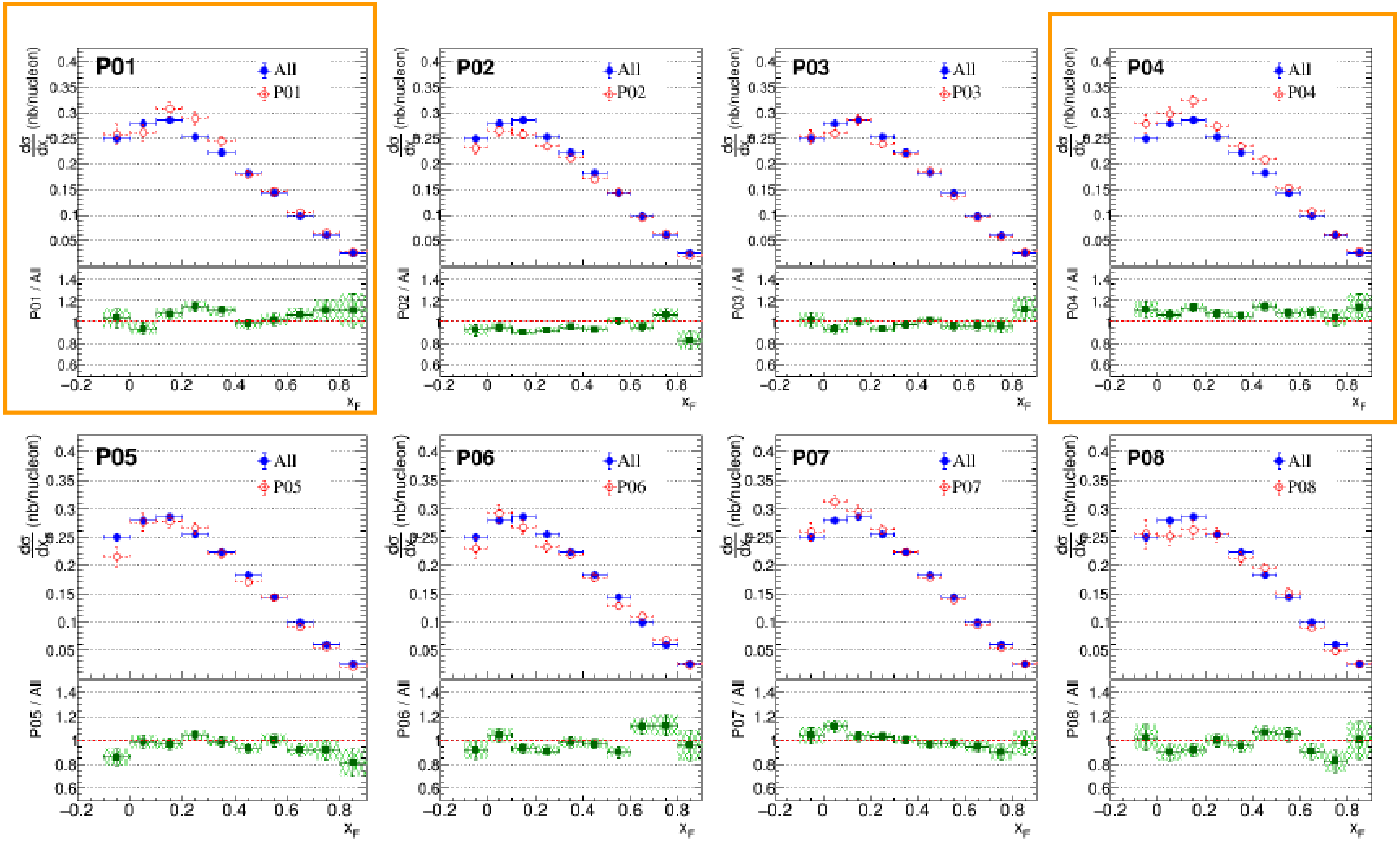

(a) *PT cells*

Systematics Uncertainty of Z_{vtx} Position

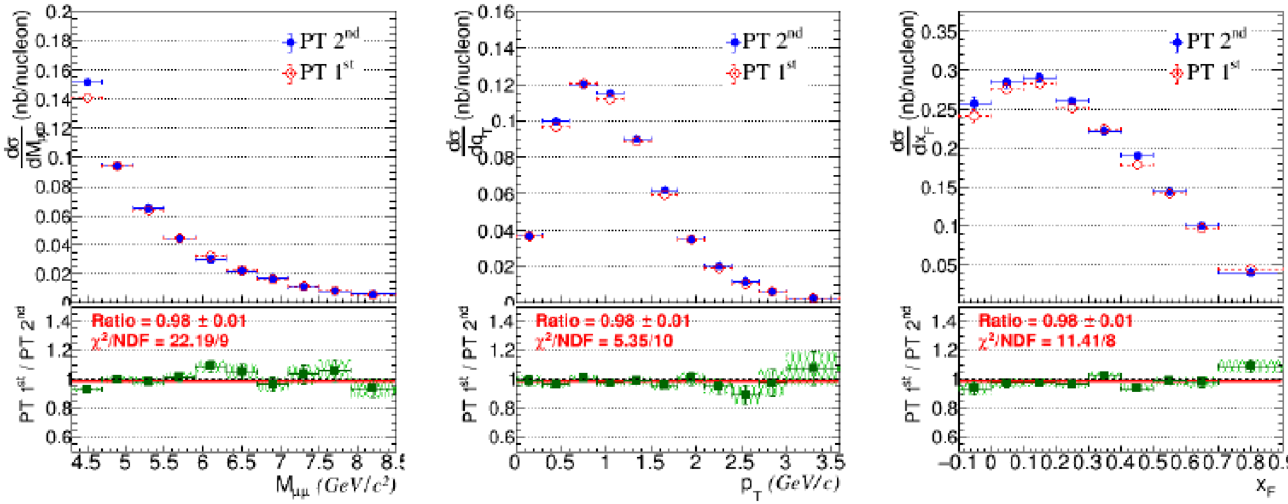

Negligible

(a) $PT\ 1^{st}\ cell/PT\ 2^{nd}\ cell$

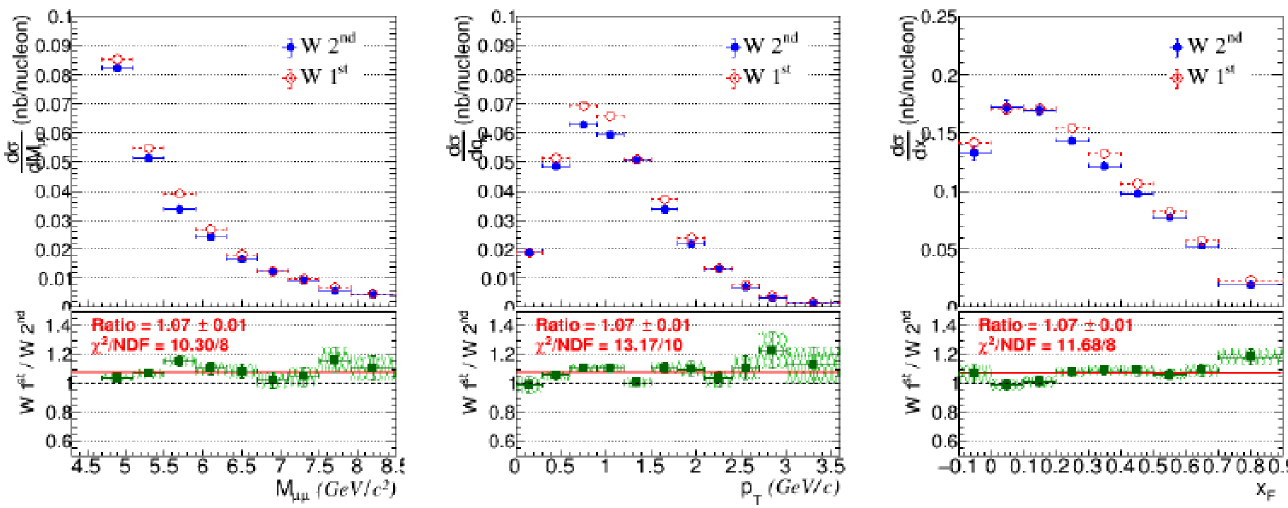

5%

(b) $W\ 1^{st}\ cell/W\ 2^{nd}\ cell$

Methods to Extract Systematics Uncertainty

- **Subsamples**
  - NH3 = [1^{st}, 2^{nd}] x [LL, LO] x [P01..P08] => 32 subsamples
  - W = [1^{st}, 2^{nd}] x [LL, LO] x [P01..P08] => 32 subsamples
  - Al = [LL, LO] x [P01..P08] => 16 subsamples

- **Methods (See details later)**
  - χ^2 method
  - Pull method

χ^2 Method

PT cells

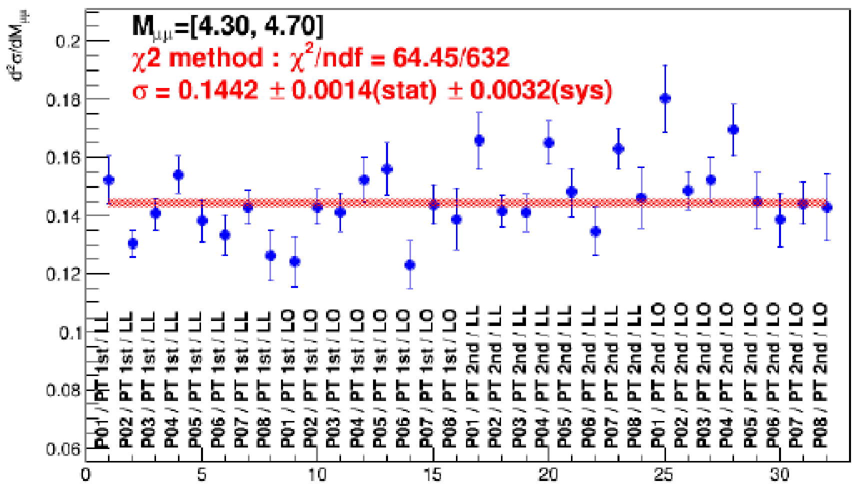

(a) $M_{\mu\mu} = [4.30, 4.70]$

- Method is used by PDG

- Example
- Use PT cells in mass bin = [4.3, 4.7] as example.
- For each bin of 3D cross-section, there are 32 subsamples. We fit data points with **pol0 function** and get chi2/ndf.
- Mean and statistical uncertainty are calculated from weighted average.

$$\bar{x} \pm \delta\bar{x}_{stat} = \frac{\sum_i w_i x_i}{\sum_i w_i} \pm \frac{1}{\sqrt{\sum_i w_i}} \quad , \quad w_i = \frac{1}{(\delta x_i)^2}$$

- Systematic uncertainty is decided by the the chi2/ndf.

(1) If chi2/ndf<=1, then data is consistent. Systematic uncertainty is zero.

(2) If chi2/ndf>1, the systematic is evaluated as follows :

$$\frac{\delta\bar{x}_{sys}}{\delta\bar{x}_{stat}} = \sqrt{\chi^2/(N-1)}$$

Bin by bin systematic uncertainty